Title
OPTICALLY DETECTED MAGNETIC RESONANCE IN ZERO FIELD

Authors
Buckley, M.J.
Harris, C.B.

Publication Date
1971-02-01

Submitted to Journal of
Physical Chemistry

UCRL-20390 Rev.
Preprint

OPTICALLY DETECTED MAGNETIC RESONANCE IN ZERO FIELD

M. J. Buckley and C. B. Harris

February 1971

AEC Contract No. W-7405-eng-48

LAWRENCE RADIATION LABORATORY
UNIVERSITY of CALIFORNIA BERKELEY

UCRL-20390 Rev.

DISCLAIMER

OPTICALLY DETECTED MAGNETIC RESONANCE IN ZERO FIELD[†]

M. J. Buckley and C. B. Harris[‡]

Department of Chemistry, University of California
Inorganic Materials Research Division, Lawrence Radiation Laboratory
Berkeley, California 94720

ABSTRACT

The dependence of the sensitivity of optically detected magnetic resonance on the intramolecular energy transfer processes is developed along with the explicit form of the spin Hamiltonian used in optically detected magnetic resonance in zero field. The main features of the optically detected ESR and ENDOR spectra in zero field for molecules with $I = 1$ and $I = 3/2$ nuclear spins is developed and illustrated by analysis of the spectra of 8-chloroquinoline in its $\pi\pi^*$ triplet state.

[†] Presented at the 2nd Symposium on Electron Spin Resonance, Athens, Georgia, 1970.

[‡] Alfred P. Sloan Fellow

I. Introduction

Since the success of optically detected magnetic resonance (ODMR) of the lowest triplet state of organic molecules is highly dependent on the nature of the triplet state, a short review of some of the important properties of the triplet state is given. There are several good review articles[1-3] (1-3) on the triplet state to which the reader is referred for a more complete discussion. The historical development of ODMR and a survey of experimental results is then given, followed by a section that deals with the sensitivity of ODMR and ENDOR in the framework of intramolecular energy transfer processes. Specifically, the effects of radiationless, radiative, and spin-lattice relaxation processes on the overall sensitivity of ODMR will be considered explicitly. The remainder of the paper will deal with the form of the spin Hamiltonian in zero-field followed by the analysis of the $\pi\pi^*$ triplet state of 8-chloroquinoline.

A. The Excited Triplet State in Organic Molecules

The ground state of most organic molecules consists of a singlet electron configuration in which all the electrons have their spins paired. The molecule may be excited to a higher energy electron configuration by the application of electromagnetic radiation of the appropriate energy. We will primarily be concerned with the excited electron configurations produced when one electron in the highest bonding molecular orbital (ϕ_A) is promoted to the lowest antibonding molecular orbital (ϕ_B). Since electrons have a spin of $\frac{1}{2}$, there are four possible orientations for the

two unpaired electrons, which, if we let α equal spin up and β equal spin down, may be represented as,

$$\begin{array}{lll} \alpha(1)\,\alpha(2) & S_z = 1 & S^2 = 1 \\ \alpha(1)\,\beta(2) & S_z = 0 & S^2 = 0 \\ \beta(1)\,\alpha(2) & S_z = 0 & S^2 = 0 \\ \beta(1)\,\beta(2) & S_z = -1 & S^2 = 1 \end{array} \qquad (1)$$

This representation, however, is not satisfactory since the electrons obey Fermi-Dirac statistics and thus the total wave function (orbital times spin) must be antisymmetric with respect to electron exchange. In addition, we would like the spin functions to be eigenstates of S^2 and S_z. The spin functions $\alpha(1)\,\alpha(2)$ and $\beta(1)\,\beta(2)$ are clearly eigenstates of S^2 and S_z since $S^2 = 1$ for both and $S_z = +1$ and -1 respectively. We can generate the $S_z = 0$ component of the triplet spin state by applying the lowering operator to the $\alpha(1)\,\alpha(2)$ state which gives us the desired spin function,

$$^3\psi_o = [1/\sqrt{2}][\alpha(1)\,\beta(2) + \beta(1)\,\alpha(2)] \qquad (2)$$

The remaining spin function is a singlet

$$^1\psi = [1/\sqrt{2}][\alpha(1)\,\beta(2) - \beta(1)\,\alpha(2)] \qquad (3)$$

and, in contrast to the triplet spin functions, is antisymmetric with respect to electron exchange. The spatial part of the excited state electron wavefunction may be represented as a symmetric (+) and antisymmetric (-) linear combination of ϕ_A and ϕ_B as:

$$\psi_{\pm} = [1/\sqrt{2}][\phi_A(1)\ \phi_B(2) \pm \phi_A(2)\ \phi_B(1)] \qquad (4)$$

Since the total wavefunction must be antisymmetric, there are only four allowed representations of the total wavefunction; a singlet state with a symmetric spatial function and an antisymmetric spin function,

$$^1\underline{\Psi} = \left([1/\sqrt{2}][\phi_A(1)\phi_B(2) + \phi_A(2)\phi_B(1)]\right)\left([1/\sqrt{2}][\alpha(1)\ \alpha(2) - \beta(1)\ \beta(2)]\right) \qquad (5)$$

and a triplet state with an antisymmetric spatial function and a symmetric spin function

$$^3\underline{\Psi} = [1/\sqrt{2}][\phi_A(1)\phi_B(2) - \phi_A(2)\phi_B(1)] \cdot \left\{ \begin{array}{l} \alpha(1)\ \alpha(2) \\ [1/\sqrt{2}][\alpha(1)\ \beta(2) + \beta(1)\ \alpha(2)] \\ \beta(1)\ \beta(2) \end{array} \right\} \qquad (6)$$

The repulsive electrostatic interaction between the two unpaired electrons gives rise to a term in the total Hamiltonian equal to e^2/r_{12}, where e is the electron charge and r_{12} is the vector connecting the two electrons. This term removes the degeneracy of the singlet and triplet states and results in the singlet state going to higher energy while the triplet state is shifted to lower energy with an energy separation between the two states of

$$^1E - {}^3E = 2\delta_{12} \qquad (7)$$

where δ_{12} is the exchange integral given by

$$\delta_{12} = \langle \phi_A(1)\phi_B(2) \mid e^2/r_{12} \mid \phi_A(2)\phi_B(1) \rangle \qquad (8)$$

For most organic molecules $2\,\delta_{12}$ is 1000 to 10000 cm^{-1}. As we will see in the discussion of the spin Hamiltonian, the inclusion of the electron dipole-dipole interaction removes the three fold degeneracy of the triplet state. This splitting is usually referred to as the zero field splitting and is on the order of 0.1 cm^{-1}. An additional contribution to the zero field splitting arises from the coupling of the spin and orbital electron angular momentum and is of the form $A(L \cdot S)$ where L and S are the spin and orbital angular momentum quantum numbers and A is a constant that depends on the particular molecule being considered. The effect of the spin-orbit Hamiltonian is to mix states of different multiplicity and, therefore, to give singlet character to triplet states and vice versa. The most important consequence of this is to permit the triplet state to undergo weak electric dipole radiation to the ground state (phosphorescence), the intensity from <u>each</u> of the three triplet sublevels being a function of the spin-orbit coupling to both the excited and ground singlet states.

Since the sensitivity of ODMR depends upon the number of molecules in their triplet state, an important consideration is intramolecular energy transfer processes. Following excitation, a molecule may lose energy by radiative or non-radiative pathways. Phosphorescence ($T_1 \rightarrow S_0$) and fluorescence ($S_1 \rightarrow S_0$) comprise the radiative pathways and proceed with rate constants on the order of 10^4 to 10^{-2} sec^{-1} and 10^6 to 10^9 sec^{-1}, respectively. The longer lifetime for phosphorescence results

from the fact that the triplet state is spin-forbidden for electric dipole radiation to the ground state.

The molecule may also lose energy through three non-radiative pathways:

1) Vibrational Relaxation -- or passage from a non-equilibrium vibrational energy distribution in a given electronic state to the Boltzmann energy distribution relative to the zero point energy of that same state. This proceeds primarily by a non-radiative mechanism with a rate constant of approximately 10^{12} sec^{-1}.

2) Internal Conversion -- or radiationless passage between two electronic states of the same spin multiplicity. This pathway also has a fast rate constant of approximately 10^{12} sec^{-1}.

3) Intersystem Crossing -- or radiationless passage from an electronic state in the singlet manifold to an electronic state in the triplet manifold or vice versa. This pathway is slower than the other two and is on the order of 10^{4} to 10^{12} sec^{-1}.

Although the exact mechanisms of intersystem crossing are not completely understood, it is generally found that at liquid helium temperatures (4.2° K) the triplet sublevels of the lowest triplet state have unequal populations because of unequal intersystem crossing rates into the individual magnetic sublevels via spin orbit and spin-vibronic coupling and unequal depopulating rates. Consequently, a state of spin alignment can exist for the electron spins.[4] The various rate constants for energy transfer, the existence of spin alignment, and the spin lattice relaxation rate between the triplet spin sublevels are all important factors in determining the sensitivity of ODMR.

(4)

B. The Historical Development of ODMR

The development of any field of science is difficult to trace since every advancement is dependent on the work of many previous researchers; however, we will choose for the starting point of this discussion the extensive study of the phosphorescence of organic molecules by Lewis and Kasha[5,6] in 1944. In their series of papers it was proposed that the phosphorescent state of these molecules corresponded to their lowest triplet state. This hypothesis was strongly supported shortly thereafter by magnetic susceptibility measurements[7,8] which showed that small changes in the susceptibility were observed upon irradiation of the samples.

As with any major change in the existing paradigm of science, this hypothesis was not universally accepted.[9] The most distressing aspect of the hypothesis was the failure to observe the predicted electron spin resonance (ESR) of the phosphorescent state. The problem was resolved in 1958 when Hutchison and Mangum[10,11] succeeded in observing the ESR of naphthalene in its phosphorescent state and showed conclusively that the phosphorescent state was a triplet state. The experiment was performed on a single crystal of naphthalene doped in durene using conventional techniques in which the absorption of the microwave energy was monitored while varying the applied magnetic field. Subsequently, the triplet state ESR of many organic compounds was observed; however, most of the work was done on randomly oriented samples. Since only one parameter can usually be measured with randomly oriented samples, the separation of the three levels of the triplet could not be determined. In certain

(12,13) cases[12,13] the three levels can be assigned but the assignment is difficult and the method has not been used often. The limited sensitivity of ESR and the difficulty of preparing single crystal samples has restricted the number of molecules investigated. Only a few (~14) molecules in single crystals have been reported to date using conventional methods and they are all characterized by relatively long lived π-π^* triplet states.

The next major change in the existing paradigm occurred in 1965 when (14) Geschwind, Devlin, Cohen and Chinn[14] reported the optical detection of the ESR of the excited metastable $\bar{E}(2E)$ state of Cr^{+3} in Al_2O_3. In this classic experiment they showed that the optical rf double resonance (15) techniques first suggested by Brossel and Kastler[15] and widely used in (16) gases[16] could also be applied to solids. The experiment was performed using a high resolution optical spectrometer to monitor the change in intensity of one of the Zeeman components of the phosphorescence [$\bar{E}$ (^1E) $\rightarrow$ $^4A_2$] as $\bar{E}$ was saturated with microwaves when the magnetic fields was swept through resonance. The resonance signal was observed by modulating the microwave field and detecting the resultant modulation of the optical emission. Since optical rather than microwave photons are detected, the sensitivity may be increased several orders of magnitude over conventional techniques. As an example, at temperatures below the λ point of helium the resonance could be observed directly on an oscilloscope without the need for phase sensitive detection. The success in optically detecting the electron spin resonance of a metastable state led several research groups to attempt to apply the same principles to

the optical detection of the ESR of organic molecules in their lowest triplet state.

In 1967 the first successful experiment was reported by Sharnoff
(17) for the $\Delta M = 2$ transition of naphthalene.[17] In this experiment a single crystal of biphenyl containing 0.1 mole percent naphthalene was placed in a microwave cavity where it was immersed in liquid helium maintained at 1.8° K. The crystal was irradiated with the appropriately filtered light from a mercury arc lamp and the phosphorescence isolated with a detector consisting of a linear polarizer and a low resolution spectrometer. The microwave field was modulated at 40 Hz and the signal detected by feeding the output of the photomultiplier into a phase sensitive amplifier. In this experiment it was shown that the radiative matrix elements connecting any triplet sublevel with the ground singlet electronic level are functions of the magnetic quantum numbers of that sublevel.

At this point the development of ODMR of the lowest triplet state of organic molecules entered a new phase. Now that this new method was shown to be applicable to these molecules the research centered around improving the basic techniques and using this new tool to gain information on the various phenomena associated with the triplet state.

(18) Shortly after Sharnoff's paper, Kwiram[18] reported the optical detection of the $\Delta M = 1$ and $\Delta M = 2$ transitions of phenanthrene in its triplet state. In this investigation the experimental methods were the same as those used by Sharnoff except that the microwave field was not modulated while the exciting and emitted light was chopped antisynchronously at 50 Hz. The 50 Hz output of the photomultiplier was converted

to DC by a phase sensitive detector and fed into a signal averager. The observed change in intensity of the phosphorescence at the three transition frequencies was used to assign the spatial symmetry of the triplet state.

(19) Schmidt, Hesselmann, De Groot and van der Waals[19] also reported the optical detection of quinoxaline (d_6) in 1967. Their experimental procedure was basically the same as that used by Sharnoff, except that they modulated the magnetic field with and without amplitude modulation of the microwave field. They were able to show (1) that the emission originates from the top spin component (out-of-plane), and (2) from phosphorescence decay studies, that entry into the triplet state by intersystem crossing is also to the top spin component.

(20) In 1968 Schmidt and van der Waals[20] extended the almost zero field
(21) work (3G) of Hutchison's group[21] by optically detecting the zero-field transitions of molecules in their triplet state at zero external magnetic field. Since it is necessary to vary the microwave frequency in order to observe the resonance in zero external magnetic field, a helix was used to couple the microwave power to the sample. The observed signals were extremely sharp and in the case of quinoxaline (d_6), showed fine structure which was tentatively explained on the basis of a first order nitrogen nuclear quadrupole and second order nitrogen hyperfine interactions. The structure was explained quantitatively in a later
(22) paper[22] in terms of a Hamiltonian incorporating these interactions.

(23) Tinti, El-Sayed, Maki and Harris[23] extended the method of optical detection in zero field by incorporating a high resolution spectrometer

and studying the effect of the microwave field on the individual lines of the phosphorescence spectrum of 2,3-dichloroquinoxaline. They showed that the use of a high resolution spectrometer will give better sensitivity in cases where there is mixed polarization of the phosphorescence, since if the total emission is monitored, the change in intensity due to the microwave field may be partially cancelled. The sensitivity was excellent, and in fact, a very strong signal was observed using C. W. conditions for both the microwave and optical radiations. The observed structure of the zero-field transitions was explained quantitatively in a later paper[24] by Harris et al., in which optically detected electron nuclear double resonance (ENDOR) was also reported. Several other papers followed on the observation and interpretation of nitrogen ENDOR in zero field[25,26] and was extended to ^{35}Cl and ^{37}Cl by Buckley and Harris.[27] Optical detection of electron-electron double resonance (EEDOR) was reported by Kuan, Tinti and El-Sayed[28] and was demonstrated to be a method of improving the signal strength of weak zero-field transitions if emission is from only one of the triplet sublevels.

As a consequence of th newness of this field most of the ODMR studies to date have been on molecules previously reported using conventional techniques. However, molecules with short triplet lifetimes which cannot be observed by conventional methods have received considerable attention and the resonances of several new molecules have been reported.

Several interesting physical phenomena result from the coupling of the triplet sublevels with a coherent microwave field.[29] Both adiabatic fast passage[30] and coherent microwave pulses[31] have been used to invert the populations of two of the triplet sublevels. It has also been proposed[29]

that microwave driven quantum beats should be observable in triplet phosphorescence in essentially the same fashion as experiments in which atomic[32] and rare earth[33] luminescence is monitored. In addition to these experiments level anticrossing[34] and transferred hyperfine and nuclear quadrupole interactions from host to guest molecules[35] has been reported.

Once of the most promising applications of magnetic resonance is the investigation of exciton interactions in crystals. Wolf and his co-workers using conventional ESR techniques have observed energy exchange between pairs of naphthalene (h_8) molecules as nearest neighbors in an isotopically dilute system,[36] and triplet excitons in pure crystals of naphthalene and anthracene single crystals.[37] Sharnoff has reported the ODMR of triplet excitons in a single crystal of benzophenone;[38] however, his results have been questioned.[34] Recently, however, Francis and Harris[39] have used ODMR to observe coherent migration of triplet Frenkel excitons in molecular crystals and have measured the density of states functions of the exciton band.

In conclusion, ODMR has developed into three basic areas: 1) the study of the electron districution of organic molecules in their triplet state by analysis of the zero field, nuclear quadrupole and hyperfine interactions, 2) investigations into the intramolecular as well as intermolecular pathways and rates of energy transfer in trap molecules by analysis of the ODMR signal as a function of time for various vibronic bands in the phosphorescence spectrum, and 3) as a tool to investigate the energy levels and dynamic properties of exciton bands in molecular crystals.

The following discussion, however, will be restricted to the first of the above areas.

II. General Considerations

A. Sensitivity Considerations in the Optical Detection of ESR

We will consider experiments performed under conditions of continuous optical excitation while monitoring the change in intensity of the phosphorescence as a function of the applied microwave field. A similar analysis of some of these processes has reciently appeared in print (see reference 40). Only the case in which the triplet state is populated by excitation of the sample into the first excited singlet state followed by intersystem crossing into the triplet state will be considered. For molecules with reasonably high symmetry (i.e., D_{2h}, C_{2h}, and C_{2v}) different modes of populating the triplet state may produce different spin alignments; however, the same considerations apply in calculating the sensitivity achieved using ODMR.

The radiative and non-radiative pathways for energy transfer are depicted in Figure 1, where $[S_1]$ is the population of the lowest excited singlet state, $[N_\chi]$ ($\chi = x,y,z$) is the steady state population of the corresponding triplet levels, $K_{1\chi}$ is the intersystem crossing rate constant from S_1 to T_1, K_χ is the radiative or phosphorescence rate constant for relaxation to S_o, K_{nx} is the non-radiative decay or relaxation rate constant from T_1 to S_o, $W_{\chi_1\chi_2}(\chi_1 \neq \chi_2)$ is the spin lattice relaxation rate constant and $P_{\chi_1\chi_2}(\chi_1 \neq \chi_2)$ is the induced rate constant due to the applied microwave field (H_1). When the microwave field does not connect any two of the zero field levels of the triplet, the steady state population is given by setting $P_{\chi_1\chi_2} = 0$. The application of the microwave field at a frequency corresponding to the energy

separation of two of the levels (i.e., $\nu = (E_x - E_y)/h$) will introduce a new pathway for relaxation causing redistribution of the population which in most cases results in a change in the phosphorescence intensity. Since optical, rather than microwave, photons are detected, one would expect the sensitivity to be improved in proportion to the ratio of the energies of the photons, which, for a typical molecule, is approximately 3×10^5. The actual change in the phosphorescence intensity, however, is a complex function of the various relaxation rate constants. Therefore, the actual improvement in sensitivity will depend on the molecule under study.

In order to derive a reasonably simple quantitative expression for the change in intensity of the phosphorescence, the three following assumptions will be made:

1) The splitting of the three triplet zero field levels by nuclear quadrupole and nuclear hyperfine interactions will be neglected,

2) Only the two levels connected by the H_1 field (τ_x and τ_y) will be considered, and

3) Only the steady state condition $dN_x/dt = dN_y/dt = 0$ will be considered for both the case when $H_1 = 0$ and $H_1 \neq 0$.

The first assumption will predict too great a change in intensity if the individual triplet levels are split by more than the frequency width of the H_1 field, since in this case the H_1 field will allow an additional relaxation pathway for only a fraction of the population of each triplet level at any given frequency. The second assumption will introduce an error in the expression for the percentage change in intensity

since the intensity contribution from the level not connected by the H_1 field (τ_z) is neglected. This assumption also requires that the spin lattice relaxation rate between τ_z and τ_x and between τ_z and τ_y be neglected. This is usually valid since the experiments are performed at or below 4.2° K. The third assumption requires that the experiment be performed using C. W. microwave conditions or modulating the microwave field with a frequency lower than the total rate constant of the system.

The differential equations describing the population of the levels shown in Figure 2 are

$$\frac{dN_x}{dt} = S_1 K_{1x} - N_x [K_{nx} + K_x + W_{xy} + P_{xy}] + N_y [W_{yx} + P_{xy}] \qquad (9)$$

$$\frac{dN_y}{dt} = S_1 K_{1y} - N_y [K_{ny} + K_y + W_{yx} + P_{xy}] + N_x [W_{xy} + P_{xy}] \qquad (10)$$

With the definitions

$$\begin{aligned} A &= K_{nx} + K_x + W_{xy} + P_{xy} \\ B &= W_{yx} + P_{xy} \\ C &= K_{ny} + K_y + W_{yx} + P_{xy} \\ D &= W_{xy} + P_{xy} \end{aligned} \qquad (11)$$

Equations 9 and 10 may be rewritten

$$\frac{dN_x}{dt} = S_1 K_{1x} - N_x A + N_y B \qquad (12)$$

$$\frac{dN_y}{dt} = S_1K_{1y} - N_yC + N_xD \tag{12}$$

The steady state assumption allows us to write

$$\frac{dN_x}{dt} = S_1K_{1x} - N_xA + N_yB = 0 \tag{14}$$

$$\frac{dN_y}{dt} = S_1K_{1y} - N_yC + N_xD = 0 \tag{15}$$

Upon solving Equations 14 and 15 for the population of the triplet levels, we have

$$N_x = \frac{S_1[CK_{1x} + BK_{1y}]}{AC - BD} \tag{16}$$

and

$$N_y = \frac{S_1[AK_{1y} + DK_{1x}]}{AC - BD} \tag{17}$$

The intensity of the phosphorescence detected with an optical spectrometer may be written

$$I = \alpha_1N_xK_x + \alpha_2N_yK_y \tag{18}$$

where α_1 and α_2 are constants that depend on the polarization of the emission, the orientation of the sample, and the efficiency of the detection system. The assumption will be made that $\alpha_1 = \alpha_2$, which allows the fractional change in the intensity of the phosphorescence upon application of the H_1 field to be written

$$\Delta I = \frac{I - I_o}{I_o} = \frac{I}{I_o} - 1 \tag{19}$$

where I_o is the intensity of the phosphorescence when $P_{xy} = 0$. With this condition, it is convenient to define the parameters given in Equation 11 as

$$\begin{aligned} a &= K_{nx} + K_x + W_{xy} \\ b &= W_{yx} \\ c &= K_{ny} + K_y + W_{yx} \\ d &= W_{xy} \end{aligned} \tag{20}$$

If both of the triplet levels are monitored, the fractional change in intensity of the emission is given by

$$\Delta I = \left\{ \frac{[K_{1y}(AK_y + BK_x) + K_{1x}(CK_x + DK_y)][ac - bd]}{[K_{1y}(aK_y + bK_x) + K_{1x}(cK_x + dK_y)][AC - BD]} \right\} - 1 \tag{21}$$

In some cases it is possible to monitor only one of the triplet levels connected by the H_1 field, in which case the change in intensity of emission from the τ_x and τ_y levels are given by

$$\Delta I_x = \left\{ \frac{[CK_{1x} + BK_{1y}][ac - bd]}{[cK_{1x} + bK_{1y}][AC - BD]} \right\} - 1 \tag{22}$$

and

$$\Delta I_y = \left\{ \frac{[AK_{1y} + DK_{1x}][ac - bd]}{[aK_{1y} + dK_{1x}][AC - BD]} \right\} - 1 \tag{23}$$

Three limiting cases will now be discussed in order to examine the effect of the magnitude of the various rate constants on the sensitivity of the experiment.

Case #1, The Effect of the Radiative Rate Constants

For this case the additional assumption is made that the non-radiative and spin lattice relaxation rate constants may be neglected. The parameters defined in Equations 11 and 20 become

$$\begin{aligned} A &= K_x + P_{xy} & a &= K_x \\ B &= P_{xy} & b &= 0 \\ C &= K_y + P_{xy} & c &= K_y \\ D &= P_{xy} & d &= 0 \end{aligned} \tag{24}$$

In the absence of the H_1 field the steady state populations are given by

$$\begin{aligned} N_x^o &= S_1(K_{1x}/K_x) \\ N_y^o &= S_1(K_{1y}/K_y) \end{aligned} \tag{25}$$

The steady state population of τ_x is given by Equation 16 which for this example becomes

$$N_x = \frac{S_1[K_{1x}K_y + P_{xy}(K_{1x} + K_{1y})]}{[K_xK_y + P_{xy}(K_x + K_y)]} \tag{26}$$

In the limit that P_{xy} is much larger than any of the relaxation rate constants, the populations of τ_x and τ_y are equalized and the transition is saturated. Clearly, the power required to equalize the populations is directly proportional to the relaxation rate of the

system and inversely proportional to the lifetime of the excited state. The population of τ_x at saturation is given by

$$N_x^s = \frac{S_1[K_{1x} + K_{1y}]}{[K_x + K_y]} \tag{27}$$

and the corresponding population of τ_y is given by

$$N_y^s = \frac{S_1[K_{1x} + K_{1y}]}{[K_x + K_y]} \tag{28}$$

and therefore, $N_x^s = N_y^s$. The change in population of τ_x upon saturation is

$$\Delta N_x = N_x^s - N_x^o = \frac{S_1[K_x K_{1y} - K_y K_{1x}]}{K_x (K_x + K_y)} \tag{29}$$

Therefore, if $K_x K_{1y} = K_y K_{1x}$, there is no change in population. If the emissions from τ_x and τ_y are monitored simultaneously, the fractional change in intensity is given by Equation 21 which, for this example, reduces to

$$\Delta I = \left\{ \frac{[K_{1y}(AK_y + BK_x) + K_{1x}(CK_x + DK_y)]}{[K_{1y}(AC - BD)]} \right\} - 1 \tag{30}$$

$$= \left\{ \frac{[K_{1x} + K_{1y}][P_{xy}(K_x + K_y) + K_x K_y]}{[K_{1x} + K_{1y}][P_{xy}(K_x + K_y) + K_x K_y]} \right\} - 1 \tag{31}$$

And therefore, $\Delta I = 0$ and no change in the intensity of emission will be observed. However, if a high resolution optical spectrometer is

used, it is often possible to monitor the emission from just one of the triplet levels via its selective emission to the origin or a vibration of the ground state singlet manifold. Consider for example, τ_x, in which case, the change in intensity given by Equation 22 becomes

$$\Delta I_x = \frac{K_x}{K_{1x}}\left[\frac{P_{xy}(K_{1x} + K_{1y}) + K_{1x}K_y}{P_{xy}(K_x + K_y) + K_xK_y}\right] - 1 \qquad (32)$$

In the limiting case where intersystem crossing proceeds primarily to τ_x $(K_{1x} \gg K_{1y})$ Equation 32 reduces to

$$\Delta I_x = \left\{\frac{P_{xy}K_x + K_xK_y}{P_{xy}(K_x + K_y) + K_xK_y}\right\} - 1 \qquad (33)$$

At saturation we have

$$\Delta I_x^s = \left(\frac{K_x}{K_x + K_y}\right) - 1 \qquad (34)$$

The effect of the ratio of the radiative rate constants (K_x/K_y) on the maximum change in intensity of the emission may be illustrated with the following examples:

K_x/K_y	ΔI_x^s (%)
0.1	91
1	50
10	9

Therefore, the maximum sensitivity is achieved if the level with the fast intersystem crossing rate constant has the slower phosphorescence rate constant. Unfortunately, the opposite is usually found to be the case.

Case #2, The Effect of Spin Lattice Relaxation

The two rate constants for spin lattice relaxation are not independent and may be related directly to the spin lattice relaxation time T_1 for any given temperature.

The interaction between the energy and the lattice may be represented schematically as

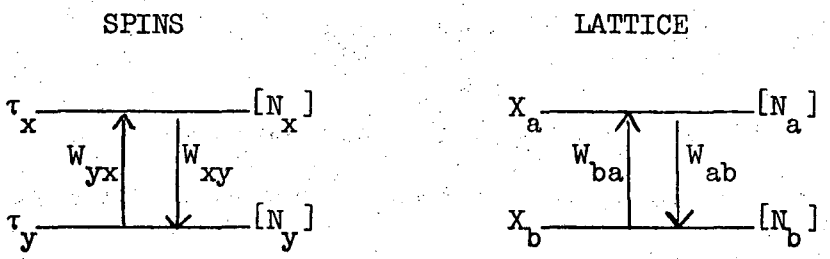

The conservation of energy requires that for each transition from τ_x to τ_y there be a corresponding lattice transition from X_b to X_a and vice versa. The transition rate for the lattice may be written

$$\begin{aligned} W_{ab} &= N_a A \\ W_{ba} &= N_b A \end{aligned} \tag{35}$$

where A is the transition probability. The spin lattice relaxation rate constants may be written in terms of the population of the lattice as

$$W_{xy} = W_{ba} = N_b A$$
$$W_{yz} = W_{ab} = N_a A \tag{36}$$

Since the lattice is at the temperature of the bath (liquid helium), the normalized population of the lattice is given by

$$N_a = \frac{e^{-\delta/2kt}}{e^{-\delta/2kt} + e^{\delta/2kt}} = f$$
$$N_b = \frac{e^{\delta/2kt}}{e^{-\delta/2kt} + e^{\delta/2kt}} = 1 - f \tag{37}$$

where $\delta = (E_x - E_y)$ and E_x and E_y are the energies of the x and y magnetic sublevels respectively. The spin lattice relaxation rates may now be written

$$W_{xy} = (1 - f)\, A$$
$$W_{yx} = (f)\, A \tag{38}$$

The spin lattice relaxation time is defined by the expression

$$T_1 = \frac{1}{W_{xy} + W_{yx}} = \frac{1}{A} \tag{39}$$

Therefore, W_{xy} and W_{yx} may be expressed in terms of T_1 and f as

$$W_{xy} = \frac{1 - f}{T_1}$$
$$W_{yx} = \frac{f}{T_1} \tag{40}$$

¶ In the derivation of Equation 40 it is assumed that only a direct process of energy transfer between the spin system and the lattice exists which is usually the case at the temperatures of the experiments (4.2° to 1.3°K). In the case that Raman or Orbach processes are present, only the explicit temperature dependence of the relaxation must be corrected so that the spin lattice relaxation may always be defined for a two level system in terms of only T_1 at a given temperature. A short T_1 relaxation time will tend to produce a Boltzmann population distribution between the spin sublevels and will therefore generally reduce the spin alignment. This can be seen by considering the simple case where there is only intersystem crossing to τ_x and emission from τ_x and τ_y. Again the non-radiative decay rate constants K_{nx} and K_{ny} are assumed to be negligible. The parameters defining this model are

$$\begin{aligned} A &= K_x + W_{xy} + P_{xy} & a &= K_x + W_{xy} \\ B &= W_{yx} + P_{xy} & b &= W_{yx} \\ C &= K_y + W_{yx} + P_{xy} & c &= K_y + W_{yx} \\ D &= W_{xy} + P_{xy} & d &= W_{xy} \end{aligned} \tag{41}$$

and the populations of τ_x and τ_y when $P_{xy} = 0$ are given by

$$N_x^o = \frac{S_1[(K_y + W_{yx})K_{1x}]}{K_xK_y + K_yW_{xy} + K_xW_{yx}} \tag{42}$$

and

$$N_y^o = \frac{S_1[(W_{xy})K_{1x}]}{K_xK_y + K_yW_{xy} + K_xW_{yx}}$$

In the limit that $W_{xy} = W_{yx} = 0$ this reduces to

$$N_x^o = \frac{S_1[K_{1x}]}{K_x}$$
$$N_y^o = 0 \qquad (43)$$

At high temperatures when $W_{xy} \approx W_{yx} \gg K_x$, K_y, K_{1x}, Equation 42 becomes

$$N_x^o = \frac{S_1[K_{1x}]}{K_x + K_y}$$
$$N_y^o = \frac{S_1[K_{1x}]}{K_x + K_y} \qquad (44)$$

Since the change in population is monitored, it is clearly advantageous to perform the experiments at the lowest possible temperature in order to decrease the thermalization of the spin levels and the resulting loss in sensitivity.

Case #3, The Effect of Non-Radiative Relaxation

The final case to be considered is the effect of the non-radiative relaxation rate constants K_{nx} and K_{ny} on the sensitivity of the experiment. It is obvious that since only the radiative emission is detected, a large rate of depopulation by non-radiative relaxation is not desirable. In the case of a sample that relaxes primarily through non-radiative pathways, the sensitivity may be improved by using conventional ESR techniques and monitoring the absorption of microwave

power, or in extreme cases by monitoring the change in temperature of the sample. A quantitative measure of the decrease in sensitivity may be calculated by substituting the appropriate rate constants into Equations 21, 22, and 23; however the expressions are rather complex and therefore not particularly useful.

It should be noted that although we have dealt with the rate processes in the discussion of sensitivity the results can be used to measure the relative rate processes associated with the individual magnetic sublevels. Specifically, the measurement of intensity changes of phosphorescence under the influence of the microwave field can yield in favorable cases the relative intersystem crossing, radiative and radiationless rate constants to and from all three magnetic sublevels. Indeed, this approach has already been applied by El-Sayed and co-
(41) workers[41] in the limit that spin-lattice relaxation may be neglected and saturation of the transition is achieved. The inclusion of the power factor, however gives one an additional experimental "handle" from which to extract information (cf. Equations 21, 22, and 23).

B. Optical Detection of ENDOR

The sensitivity of this experiment may be simply estimated if the assumption is made that there is no nuclear polarization. Since this assumption has yet to be thoroughly investigated, it is reasonable to expect that in some cases it will not be valid. Nuclear polarization may arise through cross relaxation between the electron and nuclear spin systems (the Overhauser effect), or it may be induced by saturation

of "forbidden" transitions (simultaneous electron-nuclear flips). It is also possible that selective intersystem crossing may preferentially populate a particular nuclear spin level if there is strong hyperfine coupling of the electron and nuclear wavefunctions.

In the absence of nuclear polarization, the sensitivity of the optically detected ENDOR signal may be understood by referring to Figure 3 in which the τ_x and τ_y triplet levels are now each composed of two levels. This splitting of the triplet levels is due to nuclear quadrupole and hyperfine interactions as will be discussed in the section on the spin Hamiltonian. The results obtained by considering the triplet levels as being split into only two nuclear sublevels are independent of the number of sublevels if the ESR transition connects only one nuclear sublevel in each of the two triplet levels, and the ENDOR transition connects only two nuclear sublevels in one of the triplet levels.

As has already been discussed, the sensitivity of the optical detection technique is dependent on the various relaxation pathways from the triplet state. The same considerations apply in an ENDOR experiment. Since the sensitivity of the ENDOR experiment will be referenced to the sensitivity of the ESR experiment, the explicit dependence of the triplet state populations on the various rate constants need not be specified. For the system shown in Figure 3, the phosphorescence intensity may then be written

$$I_o = 2(N_x K_x + N_y K_y) \tag{45}$$

where N_x (N_y) is now defined as the population of each of the two levels in the τ_x (τ_y) manifold.

Upon saturation of the electron spin transition $(b \leftrightarrow d)$, this becomes

$$I_S = \left(\frac{3N_x + N_y}{2}\right)K_x + \left(\frac{3N_y + N_x}{2}\right)K_y \qquad (46)$$

with the change in intensity given by

$$\Delta I = I_S - I_o = \tfrac{1}{2}(N_x - N_y)(K_y - K_x) \quad . \qquad (47)$$

If the ENDOR transition $(a \leftrightarrow b)$ is also saturated, the intensity is given by

$$I_E = \frac{2}{3}\left[(2N_x + N_y)K_x + (2N_y + N_x)K_y\right] \quad . \qquad (48)$$

Since the ENDOR signal is detected by monitoring the change in intensity of the ESR transition, the signal strength is given by

$$\Delta I_E = I_E - I_S \qquad (49)$$

$$= \frac{1}{6}\left[(N_x - N_y)(K_y - K_x)\right] \qquad (50)$$

and the fractional change in intensity of the ESR signal upon saturation of the ENDOR transition is

$$\delta I = \Delta I_E / \Delta I_S = \frac{1}{3} \quad . \qquad (51)$$

If the ENDOR transition $(c \leftrightarrow d)$ is saturated instead of the transition from $(a \leftrightarrow b)$, the same expression is obtained for the change in intensity (Equations 50 and 51).

It is interesting to note from Equations 47 and 50 that the ESR signal and the ENDOR signal always affect the intensity of the phosphorescence in the same direction.

If the forbidden ESR transition from $(b \leftrightarrow c)$ is saturated and if the two ENDOR transitions $(a \leftrightarrow b)$ and $(c \leftrightarrow d)$ occur at the same frequency, the change in phosphorescence intensity is given by

$$\Delta I_E = \frac{1}{2}\left[(N_x - N_y)(K_y - K_x)\right] \tag{52}$$

and the fractional change in intensity of the ESR signal is unity.

As a final note, if the ESR transitions from $(a \leftrightarrow c)$ and $(b \leftrightarrow d)$ occur at the same frequency, the ENDOR transitions from $(a \leftrightarrow b)$ and $(c \leftrightarrow d)$ must also occur at the same frequency causing the change in intensity of the ESR signal to be twice as large (Equation 47),

$$\Delta I = (N_x - N_y)(K_y - K_x) \tag{53}$$

while the ENDOR transitions will not be observed since the populations of the nuclear sublevels are already equal.

III. The Zero Field Spin Hamiltonian

The observed magnetic resonance spectra of the excited triplet state of organic molecules in zero external magnetic field may be understood in terms of a Hamiltonian of the form,

$$H = H_{SS} + H_Q + H_{HF}$$

where H_{SS} is the spin-spin or zero field interaction between the two unpaired electrons, H_Q is the nuclear quadrupole interaction, and H_{HF} is the nuclear electron hyperfine interaction.

A. H_{SS} -- The Spin-spin or Zero Field Splitting Hamiltonian

H_{SS} is primarily due to the magnetic dipole-dipole interaction between the unpaired electrons in the excited triplet state. There can also be a contribution from the spin orbit coupling between the lowest triplet and other excited states; however, the contribution from the interaction between other excited triplet states will shift the three levels equally, and may therefore be neglected.[42] (42)

If the radiative lifetime for fluorescence and phosphorescence is known, the magnitude of the spin-orbit contribution to the zero field splitting may be estimated by choosing a simple model in which the transition probability for phosphorescence is due only to the spin-orbit coupling of one spin sublevel with only one excited singlet state. In the framework of this model the transition probability for phosphorescence may be expressed as

$$P_P \approx |\langle {}^3\psi_1| \vec{er} |{}^1\psi_o\rangle|^2 = \frac{1}{\tau_P} \qquad (54)$$

where $\vec{er}$ is the electron dipole moment transition operator, ${}^3\psi_1$ is the first triplet state, ${}^1\psi_o$ is the ground singlet state, and τ_P is the phosphorescence radiative lifetime. The wave function for the phosphorescent triplet state is actually a linear combination of the pure triplet state, which is spin forbidden for electric dipole radiation to

the ground state, and an admixture of singlet character due to spin-orbit coupling. ${}^3\psi_1$ may therefore be represented as a linear combination of ${}^3\psi_1^o$ and ${}^1\psi_1^o$ as

$$ {}^3\psi_1 = C_1\, {}^3\psi_1^o + C_2\, {}^1\psi_1^o \tag{55} $$

where ${}^3\psi_1^o$ and ${}^1\psi_1^o$ are the wave functions for the first excited singlet and triplet states respectively in the absence of spin-orbit coupling. In organic molecules the spin orbit matrix element is generally small so $C_1 \approx 1$ while C_2 is given from perturbation theory by

$$ C_2 = \frac{\langle {}^1\psi_1^o |\ H_{SO}\ | {}^3\psi_1^o \rangle}{|{}^1E_1 - {}^3E_1|} = \frac{\delta}{|{}^1E_1 - {}^3E_1|} \quad . \tag{56} $$

where ${}^1E_1$ is the energy of ${}^1\psi_1$ and ${}^3E_1$ is the energy of ${}^3\psi_1$. The phosphorescence transition probability (Equation 54) may now be written

$$ \frac{1}{\tau_P} = \left| \langle C_1\, {}^3\psi_1^o + C_2\, {}^1\psi_1^o |\ e\vec{r}\ | {}^1\psi_o \rangle \right|^2 \tag{57} $$

$$ = C_2^2 \left| \langle {}^1\psi_1^o |\ e\vec{r}\ | {}^1\psi_o \rangle \right|^2 $$

while the fluorescence transition probability is given by

$$ P_F \approx \left| \langle {}^1\psi_1 |\ e\vec{r}\ | {}^1\psi_o \rangle \right|^2 = \frac{1}{\tau_F} \quad . \tag{58} $$

Substituting Equation 58 into Equation 57, we have

$$ C_2^2 = \frac{\tau_F}{\tau_P} = \frac{\delta^2}{|{}^1E_1 - {}^3E_1|^2} \tag{59} $$

Within the limits of the model, the spin-orbit matrix element is given by

$$\delta = \left(\frac{\tau_F}{\tau_P}\right)^{\frac{1}{2}}\left({}^1E_1 - {}^3E_1\right) \tag{60}$$

Also from perturbation theory the shift in energy of the triplet zero field level coupled to ${}^1\psi_1$ may be written

$$\Delta = \frac{\delta^2}{|{}^1E_1 - {}^3E_1|} = \left(\frac{\tau_F}{\tau_P}\right)\left({}^1E_1 - {}^3E_1\right) \tag{61}$$

(43) As an example, for benzene,[43] $\tau_P = 30$ sec, $\tau_F = 3 \times 10^{-8}$ sec, and assuming $|{}^1E_1 - {}^3E_1| \leq 6000$ cm^{-1}, we have,

$$\Delta = \frac{3 \times 10^{-8} \text{ sec}}{30 \text{ sec}} \quad (6000 \text{ cm}^{-1})$$

$$= 6 \times 10^{-5} \text{cm}^{-1}$$

(44) Compared to the measured zero field splittings of benzene[44] of 0.1644 cm^{-1}, 0.1516 cm^{-1}, and 0.0128 cm^{-1}, the spin-orbit coupling contribution to the zero field splitting is clearly negligible. The addition of a heavy atom will increase the spin orbit coupling matrix element. An example (45) of the magnitude of the effect is given by paradichlorobenzene[45] for which $\tau_P = 16$ ms., $\tau_F = 3 \times 10^{-8}$ sec, and $|{}^1E_1 - {}^3E_1| \leq 7800$ cm^{-1}. Substituting these values into Equation 61, we find that $\Delta = 1.5 \times 10^{-2}$ cm^{-1}. (46) This is still small compared to the observed zero field splittings[46] of 0.1787 cm^{-1}, 0.1201 cm^{-1}, and 0.0584 cm^{-1}. In addition, since we used

the measured lifetime of the phosphorescence which includes both the radiative and non-radiative transition probabilities, the actual contribution of spin-orbit coupling to the zero field splitting is certainly smaller. For organic molecules in their excited triplet state, the splitting of the zero field levels due to spin-orbit coupling usually accounts for only a small percentage of the observed zero field splitting and therefore, we will consider on the magnetic dipole-dipole interaction in explaining the observed spectra.

The Hamiltonian for the magnetic dipole-dipole interaction between two unpaired electrons may be written[47] as (47)

$$H_{SS} = g_e^2 \beta_e^2 \left\{ \frac{S_1 \cdot S_2}{r^3} - \frac{3(S_1 \cdot r)(S_2 \cdot r)}{r^5} \right\} \tag{62}$$

where g_e is the electron g factor, which has been found to be basically isotropic for aromatic triplet states and equal to the free electron value of 2.00232, β_e is the Bohr magneton (eh/2mc), and r is the vector connecting the two electron spins S_1 and S_2. The Hamiltonian is of the same form as any dipole-dipole interaction, and in the case of the interaction between the two triplet state electrons may be expressed as

$$H_{SS} = S \cdot D \cdot S \tag{63}$$

which may be written in a Cartesian axis system as

$$H_{SS} = D_{xx}S_x^2 + D_{xy}S_xS_y + D_{xz}S_xS_z + D_{yx}S_yS_x + D_{yy}S_y^2 + D_{yz}S_yS_z + D_{zx}S_zS_x + D_{zy}S_zS_y + D_{zz}S_z^2 \quad (64)$$

The values of the D_{ij} $(i,j = x,y,z)$ are given by averages over the triplet state electronic wave function[48] (48)

$$D_{xx} = \frac{1}{2} g_e^2\beta^2 \left\langle \frac{r^2 - 3x^2}{r^5} \right\rangle$$

$$D_{xy} = \frac{1}{2} g_e^2\beta^2 \left\langle \frac{-3xy}{r^5} \right\rangle \quad (65)$$

and so on. D is a symmetrical tensor ($D_{xy} = D_{yx}$, etc.); therefore, in the principal axis system which diagonalizes the zero field tensor, the Hamiltonian becomes

$$H_{SS} = -XS_x^2 - YS_y^2 - ZS_z^2 \quad (66)$$

where $X = -D_{xx}$, $Y = -D_{yy}$, and $Z = -D_{zz}$

Since the Hamiltonian is traceless, $X + Y + Z = 0$, only two independent parameters are needed to describe the interaction. In conventional ESR the Hamiltonian in the principal axis system is usually rewritten by defining

$$D = \frac{1}{2}(X + Y) - Z \quad \text{and} \quad E = -\frac{1}{2}(X - Y) \quad (67)$$

with the axis convention that $|X| \leq |Y| \leq |Z|$. Therefore, the three components of the Hamiltonian are given by

$$\begin{aligned} X &= D/3 - E \\ Y &= D/3 + E \\ Z &= -2/3\ D \end{aligned} \tag{68}$$

Thus, for the triplet state, the zero field spin-spin interaction can be written in diagonal form as

$$H_{SS} = D(S_z^2 - 2/3) + E(S_x^2 - S_y^2) \tag{69}$$

where the triplet electron representations X, Y, and Z are related to the S_z eigenstates by:

$$\begin{aligned} |X> &= 1/\sqrt{2}\ (|-1> - |1>) \\ |Y> &= i/\sqrt{2}\ (|-1> + |1>) \\ |Z> &= |0> \end{aligned} \tag{70}$$

This form of the Hamiltonian is directly related to the chosen axis system of the molecule and presents a clear picture of the orientational dependence of the energy.

The usual selection rule in ESR of $\Delta S_z = \pm 1$ is not valid in zero magnetic field since the triplet sublevels are not eigenfunctions of S_z. The probability of magnetic dipole transitions between the triplet spin sublevels are given by

$$\begin{aligned} P_{x\to y} &= |<X|\ S_z\ |Y>|^2 = 1 \\ P_{x\to z} &= |<X|\ S_y\ |Z>|^2 = 1 \\ P_{y\to z} &= |<Y|\ S_x\ |Z>|^2 = 1 \end{aligned} \tag{71}$$

B. H_Q -- The Nuclear Quadrupole Hamiltonian

A nucleus with a spin ≥ 1 will have a non-spherical charge distribution and therefore an electric quadrupole moment. The quadrupole moment of the nucleus may be positive or negative depending on whether the charge distribution is elongated or flattened along the spin axis. Each allowed nuclear orientation along the spin axis will have associated with it a potential energy due to the surrounding electric field. In the case of a free molecule, the electric field is due to non-s electrons which produce a field gradient ($V_{i,j}$) at the nucleus defined by

$$V_{i,j} = \frac{\partial^2 V}{\partial_i \, \partial_j} \quad (i,j = x,y,z) \tag{72}$$

where V is the electrostatic potential at the nucleus.

(49) In an arbitrary axis system the Hamiltonian[49] may be written as

$$\begin{aligned} H_Q = B \Big\{ & V_{zz}(3I_z^2 - I^2) + (V_{zx} + i\,V_{zy})(I_- I_z + I_z I_-) \\ & + (V_{zx} - i\,V_{zy})(I_+ I_z + I_z I_+) + [1/2(V_{xx} - V_{yy}) \\ & + i\,V_{xy}]\, I_+^2 + [1/2(V_{xx} - V_{yy}) - i\,V_{xy}]\, I_-^2 \Big\} \end{aligned} \tag{73}$$

where $B = \dfrac{eQ}{4I(2I-1)}$

e = the electron charge (esu)

Q = the quadrupole moment (cm^2)

and I = the nuclear spin quantum number.

The Hamiltonian is a symmetric tensor and by transforming to an axis system such that $V_{i,j} = 0$ for $i \neq j$, the Hamiltonian may be rewritten as:

$$H_Q = B\left\{V_{zz}(3I_z^2 - I^2) + [1/2(V_{xx} - V_{yy})(I_+^2 + I_-^2)]\right\} . \quad (74)$$

Since the Hamiltonian only includes interactions due to charges external to the nucleus, the Laplace equation is satisfied and therefore:

$$V_{xx} + V_{yy} + V_{zz} = 0 . \quad (75)$$

Consequently, it is only necessary to specify two independent parameters to describe the interaction. The conventional nomenclature in nuclear quadrupole resonance spectroscopy defines the field gradient, q, and the asymmetry parameter, η, by the relations

$$\begin{aligned} eq &= V_{zz} \\ \eta &= \frac{V_{xx} - V_{yy}}{V_{zz}} \end{aligned} \quad (76)$$

with the convention

$$|V_{xx}| \leq |V_{yy}| \leq |V_{zz}| \quad (77)$$

The standard form of the Hamiltonian, Equation 74, may now be written as

$$H_Q = A\left[(3I_z^2 - I^2) + \eta/2\,(I_+^2 + I_-^2)\right] \quad (78)$$

where $A = \frac{e^2qQ}{4I(2I-1)}$.

This may also be written in the completely equivalent form

$$H_Q = A\left[(3I_z^2 - I^2) + \eta\ (I_x^2 - I_y^2)\right] \quad . \tag{79}$$

The Hamiltonian matrix therefore consists of diagonal terms and off diagonal terms connecting states differing in I_z by ± 2.

At this point we will consider the explicit form of the Hamiltonian for $I = 1$ and $I = 3/2$ since interactions due to both spins were observed in the course of this work.

The Hamiltonian for an $I = 1$ nucleus may be expressed in a more convenient form by transforming Equation 79 to the representation in which the energy is diagonal. In this representation the Hamiltonian is in the same form as the spin-spin Hamiltonian, and is particularly convenient since it may be written in terms of the nuclear angular momentum operators as

$$H_Q = -xI_x^2 - yI_y^2 - zI_z^2 \tag{80}$$

which is in the same form as the zero field Hamiltonian (Equation 66).

For a spin of $I = 3/2$ it is more convenient to use matrix notation. The Hamiltonian matrix for $I = 3/2$ may be written as

$$H_Q = \frac{e^2qQ}{4} \cdot \tag{81}$$

	$\lvert 3/2 \rangle$	$\lvert 1/2 \rangle$	$\lvert -1/2 \rangle$	$\lvert -3/2 \rangle$
$\langle 3/2 \rvert$	1	0	$\eta/\sqrt{3}$	0
$\langle 1/2 \rvert$	0	-1	0	$\eta/\sqrt{3}$
$\langle -1/2 \rvert$	$\eta/\sqrt{3}$	0	-1	0
$\langle -3/2 \rvert$	0	$\eta/\sqrt{3}$	0	1

The matrix may be rewritten as two separate 2 x 2 matrices by re-arranging the order of the basis states as

$$H_Q = \frac{e^2qQ}{4} \cdot \begin{array}{c|c|c|c} |3/2> & |-1/2> & |1/2> & |-3/2> \\ \hline 1 & \eta/\sqrt{3} & 0 & 0 \\ \hline \eta/\sqrt{3} & -1 & 0 & 0 \\ \hline 0 & 0 & -1 & \eta/\sqrt{3} \\ \hline 0 & 0 & \eta/\sqrt{3} & 1 \end{array} \tag{82}$$

The eigenvalues of the Hamiltonian may now be obtained by diagonalizing each of the 2 x 2 matrices with the result that there are only two energy levels, both of which are doubly degenerate

$$\begin{aligned} E_{\pm 3/2} &= \frac{e^2qQ}{4}\left(1 + \eta/3\right)^{1/2} \\ E_{\pm 1/2} &= \frac{-e^2qQ}{4}\left(1 + \eta/3\right)^{1/2} \end{aligned} \tag{83}$$

The eigenstates are

$$\begin{aligned} |3/2>' &= a|3/2> + b|-1/2> \\ |-1/2>' &= a|-1/2> - b|3/2> \\ |1/2>' &= a|1/2> - b|-3/2> \\ |-3/2>' &= a|-3/2> + b|1/2> \end{aligned} \tag{84}$$

where

$$a = \frac{1 + \sqrt{1 + x^2}}{[2(1 + x^2 + \sqrt{1 + x^2})]^{1/2}} \tag{85}$$

$$b = x/\left[2(1 + x^2 + \sqrt{1 + x^2}\right]^{1/2}$$

and $$x = \eta/3$$

In contrast to a nucleus with spin $I = 1$, we cannot determine both e^2qQ and η by measuring only the transition energy since the levels are twofold degenerate. It is therefore necessary to apply a perturbation such as a Zeeman field to remove the degeneracy of the $\pm$ levels in order to completely measure the nuclear quadrupole interaction. It should be noted, however, that the transition frequency is not particularly sensitive to η. The assumption that $\eta = 0$ and therefore that the transition energy is equal to $(1/2)e^2qQ$ will produce only a small error for small values of η. Furthermore, an oscillating magnetic field along the Z axis will not induce magnetic dipole transitions between the $\pm 3/2$ and $\pm 1/2$ nuclear levels if $\eta = 0$.

C. H_{HF} -- The Nuclear Electron Hyperfine Interaction

A nucleus with a spin $\geq 1/2$, like an electron, will have a magnetic moment. The interaction of this nuclear magnetic moment, with the electron magnetic moment, will lead to both an anisotropic dipole-dipole interaction and the Fermi contact interaction due to a finite electron spin density at the nucleus.

The component of the hyperfine interaction, due to the interaction of the nuclear and electron magnetic moments, is entirely analogous to the zero field Hamiltonian with the replacement of one of the electron

spins with a nuclear spin and the appropriate change of constants. The Hamiltonian[48] may be written as

$$H_{HF}^{DD} = - g_e \beta_e g_n \beta_n \left[\frac{I \cdot S}{r^3} - \frac{3(I \cdot r)(S \cdot r)}{r^5} \right] \tag{86}$$

and g_n is the nuclear g factor and β_n is the nuclear magneton. Since this is identical in form to Equation 62 for the zero field Hamiltonian, Equation 86 may be expressed as

$$H_{HF}^{DD} = S \cdot A \cdot I \tag{87}$$

which may be expanded in the same manner as Equation 64. The A matrix is symmetric and therefore, in its principal axis system, may be written as,

$$H_{HF}^{DD} = A_{xx} S_x I_x + A_{yy} S_y I_y + A_{zz} S_z I_z \tag{88}$$

where the hyperfine elements are given by the average over the spatial distribution of the unpaired spins

$$A_{\chi\chi} = - g_e g_n \beta_e \beta_n \left\langle \frac{r^2 - 3\chi^2}{r^5} \right\rangle \tag{89}$$

where $\chi = x, y, z$.

The Laplace equation is again satisfied and therefore,

$$A_{xx} + A_{yy} + A_{zz} = 0 \quad . \tag{90}$$

The unpaired spin density at the nucleus will produce an additional contribution to the hyperfine Hamiltonian, the Fermi contact term.

This will arise only from spin density in s orbitals since the other orbitals have a vanishing probability of being at the nucleus. The Fermi contact contribution is usually considered to be isotropic and may therefore be written as

$$H_{HF}^{F} = C(S_x I_x + S_y I_y + S_z I_z) \tag{91}$$

where

$$C = (8\pi/3)\gamma_e \gamma_n \hbar^2 |\psi_s(0)|^2 \tag{92}$$

and $|\psi_s(0)|^2$ is the s electron spin density at the nucleus.

The total hyperfine Hamiltonian may now be written as

$$H_{HF} = A'_{xx} S_x I_x + A'_{yy} S_y I_y + A'_{zz} S_z I_z \tag{93}$$

where

$$A'_{xx} = A_{xx} + C, \text{ etc.} \tag{94}$$

Therefore, if the three components of the total hyperfine Hamiltonian are measured, the contribution due to the anisotropic and isotropic components can be separated; however, the absolute signs will not generally be obtained. It should be pointed out that since the nuclei in which we are interested also have quadrupole moments, the Fermi contact term will not be strictly isotropic since the nuclei are distorted, and consequently, the dipole-dipole and contact terms are not completely separable.

D. The Total Hamiltonian, Energy Levels and Transition Probabilities

In this section the total Hamiltonian for two molecules which are examples of the triplet state electrons interacting with an $I = 1$ and

an $I = 3/2$ nuclear spin will be considered. In order to simplify the discussion we will make the following assumptions for both cases:

1) The principal axis system of H_{SS}, H_Q and H_{HF} are coincident,
2) Only the out-of-plane component of the hyperfine Hamiltonian need be considered, and
3) The hyperfine interaction due to protons may be neglected.

Assumptions 1 and 2 can be, in many cases, justified on the basis of the single crystal ESR spectra,[50] and assumption 3 (50)
on the fact that resolved proton hyperfine splitting has not been observed in zero field ESR.

An example of a molecule which is characterized by the interaction of one $(I = 1)$ nuclear spin with the triplet electrons is the $\pi\pi^*$ state of quinoline (1-azanaphthalene). The spin Hamiltonian for this molecule may be written as

$$H = H_{SS} + H_Q + H_{HF} \tag{95}$$

where

$$\begin{aligned} H_{SS} &= -XS_x^2 - YS_y^2 - ZS_z^2 \\ H_Q &= -xI_x^2 - yI_y^2 - zI_z^2 \end{aligned} \tag{96}$$

and

$$H_{HF} = A_{xx} S_x I_x$$

where x is the out-of-plane axis.

For illustration[51] (51)
we will use for the basis states the product functions $|\mu\ \nu> = \tau_\mu\ \chi_\nu$, which form a set of eigenfunctions that

diagonalize H_{SS} and H_Q. τ_μ and χ_ν are the electron and nuclear spin function while μ and ν correspond to x,y and z.

The complete Hamiltonian is of course a 9 x 9 matrix. Since we are only considering the A_{xx} element of the hyperfine interaction,[50] a satisfactory solution is obtained by perturbation theory. As is shown in Figure 4, the energy of the states $|Zz>$ and $|Zy>$ are shifted by an amount β, where

$$\beta = \frac{A_{xx}^2}{E_y - E_z} \tag{97}$$

while the states $|Yz>$ and $|Yy>$ are shifted by an amount $-\beta$.

In our axis system the triplet state energy levels would be ordered $Z > Y > X$ and the nuclear quadrupole energy levels ordered $x > z > y$. The eigenvectors of the states which are coupled by A_{xx} are

$$\begin{aligned}
|Zz>' &= (1 - \beta)\ |Zz> - \beta\ |Yy> \\
|Zy>' &= (1 - \beta)\ |Zy> - \beta\ |Yz> \\
|Yz>' &= (1 - \beta)\ |Yz> + \beta\ |Zy> \\
|Yy>' &= (1 - \beta)\ |Yy> + \beta\ |Zz>
\end{aligned} \tag{98}$$

The probability for microwave transitions between the triplet state magnetic sublevels is given by

$$I \approx |<\mu_1 \nu_1 | H_{RF}(t) | \mu_2 \nu_2>|^2 \tag{99}$$

where $H_{RF}(t)$ is the magnetic dipole transition operator defined by

$$H_{RF}(t) = H_1(t)\ \hbar\ (\gamma_n \cdot I + \gamma_e \cdot S) \tag{100}$$

and $H_1(t)$ is the magnitude of the time dependent magnetic field.

The electron spin magnetic dipole transition operator will connect states with $\mu_1 \neq \mu_2$ and $\nu_1 = \nu_2$, while the nuclear spin operator will connect states with $\mu_1 = \mu_2$ and $\nu_1 \neq \nu_2$. However, the mixing of the basis function by A_{xx} allows the observation of "forbidden" simultaneous electron and nuclear transitions. This is clearly shown by considering the transition from $|Xz>'$ to $|Yy>'$. The intensity of the transition is given by

$$I \approx |<Xz|\gamma_e H_1(t)|[(1-\beta)|Yy> + \beta|Zz>]|^2 \qquad (101)$$

$$I \approx \beta^2 \gamma_e{}^2 H_1(t)^2 \qquad (102)$$

It should be noted that it is necessary to have a hyperfine interaction in order to observe the nuclear quadrupole satellites since the hyperfine term is the only method of coupling the electron and nuclear spin Hamiltonians.

In Figure 5, the spectra expected for the three zero field transitions are shown in terms of the components of the total Hamiltonian. It is clear that the separation of the quadrupole satellites for both the $\tau_x \rightarrow \tau_z$ and $\tau_x \rightarrow \tau_y$ transitions is $2(z - y)$ and therefore only one of the three possible nuclear quadrupole transitions equal to $(3/4)\, e^2qQ\,(1 - \eta/3)$ is observed. The value of the hyperfine coupling constant A_{xx} is easily obtained from the separation of the two allowed components of each of the three transitions. If we had

chosen to use A_{yy} or A_{zz} as the only hyperfine interaction instead of A_{xx}, the spectra would be the same as that shown in Figure 5 if a cyclic perturbation is applied to our labeling.

Although in this simple example all the parameters in the Hamiltonian can be determined from the three zero field transitions, in practice this is usually not the case. This can be due to such problems as poor resolution of the spectra or the failure to include enough terms in the Hamiltonian to adequately describe the interactions. Therefore, it is usually advantageous to also perform an electron nuclear double resonance (ENDOR) experiment to improve the resolution and confirm the assignment of the spectra. The ENDOR transitions are shown in Figure 4 by the double arrows.

Because spectra have been assigned incorrectly by failing to consider the proper form of the magnetic dipole transition operator,[22] let us consider the intensity of the ENDOR transition. As an example we will treat the transition from $|Yy>'$ to $|Yz>'$

$$I \approx \left|\left[(1-\beta)<Yy|+\beta<Zz|\right]\right| H_{RF(t)} \left|\left[(1-\beta)|Yz>+\beta|Zy>\right]\right|^2 \quad (103)$$

$$I \approx \left[(1-\beta)^2 \gamma_n H_1 + 2\beta(1-\beta)\gamma_e H_1 + \beta^2 \gamma_n H_1\right]^2 \quad (104)$$

Since H_1 is a constant, we will drop it and may now write

$$I \approx 4\gamma_e^2\left[\beta^2(1-\beta)\right] + 4\gamma_e\gamma_n\left[\beta(1-\beta)^3 + \beta^3(1-\beta)\right] + \gamma_n^2\left[(1-\beta)^4 + \beta^4 + 2\beta^2(1-\beta)^2\right] \quad (105)$$

Since β is usually on the order of 1×10^{-2} for $\pi\pi^*$ triplets, we can reasonably approximate Equation 64 by

$$I \approx 4\beta^2 \gamma_e^2 + 4\beta \gamma_e\gamma_n + \gamma_n^2 \qquad (106)$$

In contrast, if there were no hyperfine coupling as in the τ_x manifold in our example, the intensity would be given by

$$I \approx \gamma_n^2 \quad . \qquad (107)$$

Therefore, the ratio of the intensity of the ENDOR transitions due to the electron magnetic dipole operator to those due to the nuclear magnetic dipole operator is approximately $4\beta^2 \gamma_e^2/\gamma_n^2$ and therefore, unless γ_n^2 is greater than $4\beta^2\gamma_e^2$ the electron dipole moment transition operator will be the major source of the intensity in ENDOR transitions.

As an example, for ^{14}N the ratio of $\gamma_e/\gamma_n = 8.6 \times 10^6$ and therefore, β must be less than 1.57×10^{-3} for the nuclear magnetic dipole transition operator to be comparable to the electron magnetic dipole transition operator in producing intensity in the ENDOR transitions. For a typical separation of $\tau_z - \tau_y$ of 1000 MHz this would correspond to an extremely small hyperfine element, A_{xx} of only 1.5 MHz, which is much smaller than any out-of-plane hyperfine elements reported for aza-aromatics.

Next, as an example of a molecule with one I = 3/2 nuclear spin we will conside the $\pi\pi^*$ state of chlorobenzene. The spectrum produced in this case is somewhat more complicated to calculate because of the lack of a convenient

basis set for both the electron and nuclear spin functions. The simplest method with only one hyperfine component is to use the basis set $|\mu\ \nu\rangle = \tau_\mu\ \chi_\nu$ where μ corresponds to X, Y and Z and ν to 3/2, 1/2, -1/2 and -3/2. We will further assume that $\eta = 0$ and therefore both H_{SS} and H_Q are again diagonal. In this example the out-of-plane component of the hyperfine tensor (A_{xx}) couples the basis states in the τ_z manifold with those in the τ_y manifold for which the nuclear spins differ in their I_z quantum number by ± 1. This is easily seen by expanding the hyperfine Hamiltonian as

$$A_{xx} S_x I_x = 1/2\left[A_{xx} S_x (I_+ + I_-)\right] \quad . \tag{108}$$

The states in the Hamiltonian that are coupled by A_{xx} may be represented graphically as

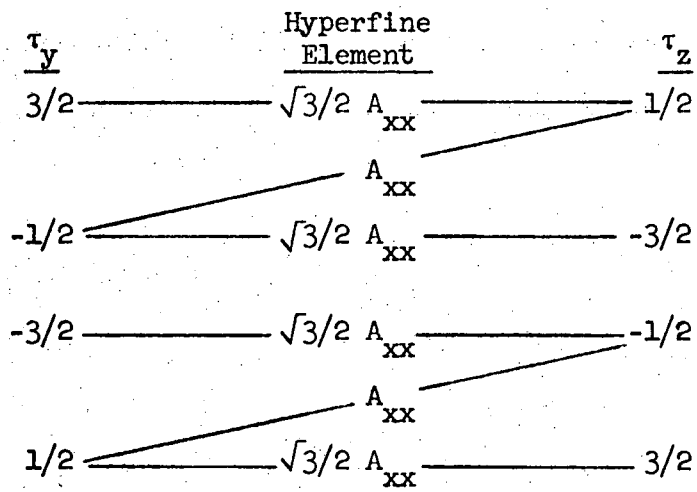

Since the degenerate nuclear levels are not coupled by the same hyperfine element, we may still use non-degenerate perturbation theory to calculate the energy levels and transition moments.

Since this spin system has a total spin that is a half integer (5/2), it is a Kramers doublet, and therefore all the energy levels are two-fold degenerate. The hyperfine coupling therefore, will never remove the degeneracy of the $\pm$ nuclear levels in zero field and consequently we have only six levels to consider.

The energy level diagram resulting from a perturbation treatment of the hyperfine interaction is given in Figure 6, and the predicted spectra in Figure The use of the A_{yy} component of the hyperfine tensor instead of the A_{xx} component produces an identical energy level diagram and spectra with the appropriate relabeling. The use of the A_{zz} component of the hyperfine tensor mixes the nuclear sublevels in the τ_x manifold with those in the τ_y manifold having the same I_z quantum number,

τ_x	Hyperfine Element	τ_y
3/2	3/2 A_{zz}	3/2
1/2	1/2 A_{zz}	1/2
-1/2	-1/2 A_{zz}	-1/2
-3/2	-3/2 A_{zz}	-3/2

therefore, no nuclear quadrupole satellites due to the electron magnetic moment transition operator are observed. The resulting energy level diagram, considering only the A_{zz} component of the hyperfine tensor is given in Figure 8 and the predicted spectra in Figure 9.

The ENDOR transitions permitted by the electron dipole moment transition operator, considering only the A_{xx} hyperfine element,

are shown by the double arrows in Figure 6. The analysis of the ENDOR spectra follows the same method as that for a spin one nucleus, with the same expression for the intensity of the transitions induced by the electron magnetic dipole moment transition operator and the nuclear magnetic dipole moment transition operator. When only the A_{zz} hyperfine element is present, the electron magnetic dipole transition operator is ineffective in producing ENDOR transitions and consequently the intensity of any observed ENDOR signal is due solely to the nuclear magnetic dipole transition operator.

Some generalizations can be made at this point concerning the appearance of "forbidden" satellites whose separation is in zeroth order is the pure nuclear quadrupole transition frequency of the molecule in an excited triplet state. (a) For a nuclear spin $I = 1$ (e.g. ^{14}N) a hyperfine element associated with a direction i, A_{ii}, gives intensity into a simultaneous electron-nuclear flip in the plane normal to i. Thus, at least two nuclear hyperfine elements must be finite to obtain independently both e^2qQ and η. (b) For a nuclear spin $I = 3/2$ (e.g. ^{35}Cl), a nuclear hyperfine element parallel to the principal axis of the field gradient (i.e., A_{zz}) does not introduce mixing between electron-nuclear states that admit intensity into forbidden satellites. (c) For a nuclear spin $I = 3/2$, a nuclear hyperfine element perpendicular to the principal axis of the field gradient introduces intensity into forbidden satellites whose separation in zeroth order is the pure nuclear quadrupole transition frequency; however, e^2qQ and η can never be obtained independently in the absence of an external magnetic field.

Although we have not treated explicitly the case where two nuclei are present on the same molecule, both having nuclear spin $I \geq 1$, the generalizations (a)-(c) hold with one additional feature being manifested, that is the possibility of simultaneous multiple nuclear-electron spin flips. As we will see in the following sections, in 8-chloroquinoline, simultaneous chlorine-nitrogen electron spin transitions are observed and are easily identified. In addition simultaneous multiple nuclear ENDOR transitions are expected and, indeed, observed.

IV. The ODMR Spectra of 8-chloroquinoline

The zero field spectra of 8-chloroquinoline is characterized by the interaction of the triplet electrons with both a nitrogen (I=1) and a chlorine (I=3/2) nucleous. The addition of the chlorine atom to quinoline does not appreciably change the lifetime of the phosphorescence (see Table 1). Both quinoline and 8-chloroquinoline show emission primarily from only one of the triplet sublevels and have essentially the same zero field, nitrogen quadrupole and nitrogen hyperfine interactions.

Although a great deal of information concerning the pathway of intramolecular energy transfer (i.e., intersystem crossing, radiative rate processes, etc.) can be obtained from an analysis of the microwave-induced phosphorescence intensity changes, we will restrict the results and discussion to the salient features of the ODMR spectra in zero field.

A. Experimental

The basic experimental arrangement is shown in Figure 10. A single crystal of 8-chloroquinoline doped in durene ($\sim 10^{-3}$ mole/mole) is mounted
(50) inside a helical slow wave structure[50] which is attached to a rigid stainless steel coaxial line suspended in a liquid helium dewar. The exciting light is supplied by a 100-watt mercury short arc lamp. The spectral region of interest selected by either an interference filter centered at 3100 Å,
(51) or a combination of Corning glass and solution filters.[51]

The phosphorescence at a 90 degree angle to the exciting light is focused through an appropriate Corning filter (to remove scattered light) and onto the entrance slit of a Jarrel-Ash model 48-490, 3/4 meter spectrometer.

The light at the exit slit is detected with a EMI 6256S photomultiplier cooled to -20°C. The output of the photomultiplier is connected to an electrometer through an adjustable load resistor. The output of the electrometer is either monitored directly if c.w. microwave power is used, or if the microwave field is amplitude modulated, connected to the signal channel input of a PAR model HR-8 lock-in amplifier.

The microwave field is generated by a Hewlett Packard microwave sweep oscillator Model 8690B, amplified with a traveling wave tube and fed consecutively through a directional coupler, band-pass filter, and an isolator to the rigid coaxial line to which the helix is mounted.

The microwave sweep oscillator may be amplitude modulated with a square wave generator which is also connected to the reference channel of the lock-in amplifier. The output of the lock-in amplifier

drives the y axis of an x - y recorder while the ramp voltage from the microwave sweep oscillator drives the x axis.

The ENDOR experiment is performed by applying an additional radio-frequency field. This is achieved by use of a Hewlett Packard radio frequency sweep oscillator model 8601A, the output of which is modulated by a linear gate and amplified by two broad band distributive amplifiers. The output of the final amplifier is applied to the ENDOR coil which consists of a bridge T constant resistance network in a Helmholtz arrangement.

The EEDOR experiment is performed by combining the output of two microwave oscillators which are isolated from each other into the same helix.

The temperature of the sample is lowered to approximately 1.3°K by pumping on the liquid helium.

B. Results

Two of the three electron spin transitions, those associated with the $\tau_z \rightarrow \tau_y$ and $\tau_x \rightarrow \tau_y$ manifolds were observed with both a continuous microwave field while monitoring the intensity of the phosphorescence and with 5 Hz amplitude modulation of the microwave field and phase sensitive detection of the component of the phosphorescence at the modulation frequency.

The $\tau_x \rightarrow \tau_z$ transition was only observed while performing an EEDOR experiment. This was performed by simultaneously saturating the $\tau_x \rightarrow \tau_y$ transition with a c.w. microwave field and amplitude modulation of a

second microwave field which was swept through the $\tau_x \rightarrow \tau_z$ transition. This was necessary since emission originates almost entirely from only the τ_y spin manifold.

In all cases the phosphorescence intensity increased when the microwave field coupled the respective electron spin manifolds.

The lifetime of the emission from the τ_y manifold was found to be 0.11 seconds while the lifetimes of both τ_x and τ_z levels are each more than one second. With the assumption that the radiative lifetimes of the triplet levels are ordered the same as the total lifetimes and the observation that the phosphorescence intensity increased while saturating both the $\tau_x \rightarrow \tau_y$ and $\tau_z \rightarrow \tau_y$ spin manifolds, from Equation 47 the steady state population of the τ_y level must be less than the population of either the τ_x or the τ_z levels.

The spectra obtained with amplitude modulation of the three ESR transitions are shown in Figure 11. At low microwave powers only the "allowed" component of each spectrum was observed. As the microwave power was increased, "forbidden" satellites split off the major transition were observed.

The ^{35}Cl ENDOR resonance observed while saturating the $\tau_z \rightarrow \tau_y$ transition is shown in Figure 12. This transition was also observed with both a continuous and amplitude modulated rf field.

C. Discussion

The essential features of the ODMR of 8-chloroquinoline have been previously reported.[27] It has subsequently been reported[52] that the (52)

phosphorescence of 8-chloroquinoline in durene is due to the two distinct sites, the more intense phosphorescence origin at 4795 Å and a weaker origin at 4792 Å. In order to isolate the emission from the site at 4795 Å, the ODMR spectra were obtained with the entrance slit of the spectrometer adjusted to 100 microns or less.

The ODMR spectra observed may be considered as due to two distinct molecular isotopes since approximately 75% of the 8-chloroquinoline molecules will have the ^{35}Cl isotope and 25% the ^{37}Cl isotope.

We will initially limit our consideration to only the 8-chloroquinoline molecules that have the ^{35}Cl isotope. The molecular axis system we will use is defined with x, the out-of-plane axis; y, the long in-plane axis; and z, the short in-plane axis.

In order to simplify the analysis of the spectra we will make the following assumptions.

1) The contribution of the proton hyperfine interaction will be neglected.

2) The principal axis systems of the spin-spin, nuclear quadrupole, and hyperfine interactions are coincident.

3) Only the out-of-plane hyperfine element for both nitrogen and chlorine will be considered.

4) The chlorine asymmetry parameter is assumed to be zero.

The first assumption is justified on the basis of the small contribution to the line width reported by Hutchison et al.[53] (53) due to the proton hyperfin interaction in zero field. This effect is smaller than the other terms in the Hamiltonian and would require an extensive computer analysis and excellent resolution of the transitions to justify its consideration, which is beyond the scope of this investigation.

The second assumption is quite severe, but is reasonable for our purposes since slight non-coincidence of the tensor elements will only produce a small perturbation of the observed spectra in zero field.

In addition, the x axis is fixed by symmetry to be perpendicular to the plane and in quinoline it has been found that the z axis of H_{SS} is within a few degrees of the molecular z axis.[54,55] It is also reasonable to expect the principal nuclear quadrupole axis for both the nitrogen and chlorine atoms to be along the molecular z axis.[49]

The third assumption is based on the measured value for the nitrogen hyperfine interaction for the excited triplet state of quinoline for which $A_{xx} \gg A_{yy}, A_{zz}$,[54] and on the observation of chlorine hyperfine interactions in organic free radicals in which the principal chlorine hyperfine element has been found to be the out-of-plane element.[56,57] In addition, since in zero field the hyperfine interaction is an off-diagonal term in the spin Hamiltonian, the magnitude of the effect of the interaction on the observed spectra is in first order inversely proportional to the energy separation of the triplet manifolds that are connected by the respective hyperfine element. Therefore, in the case of 8-chloroquinoline even if the hyperfine interaction was isotropic, the effect on the zero field spectra would still be three times larger for the A_{xx} than the A_{yy} or A_{zz} components. Therefore, only the A_{xx} component of the hyperfine tensor will be included for both the chlorine and nitrogen atoms since this will account for the major features of the spectra.

The fourth assumption is made on the basis that a finite value of the chlorine asymmetry parameter is a small perturbation that is not easily resolvable and not necessary to explain the main features of the spectra.

With these assumptions, the spin Hamiltonian may be written

$$H = H_{SS} + H_Q^N + H_{HF}^N + H_Q^{Cl} + H_{HF}^{Cl} \qquad (109)$$

where

$$\begin{aligned} H_{SS} &= -XS_x^2 - YS_y^2 - ZS_z^2 \\ H_Q^N &= -xI_x^2 - yI_y^2 - zI_z^2 \\ H_{HF}^N &= A_{xx}^N(S_xI_x) \\ H_Q^{Cl} &= \frac{e^2qQ}{12}\left[3I_z^2 - \frac{15}{4}\right] \\ H_{HF}^{Cl} &= A_{xx}^{Cl}(S_xI_x) \end{aligned} \qquad (110)$$

In the same manner as discussed in section III-D the basis states of the spin Hamiltonian are chosen to be the product functions $|u,v,w> = \tau_u, \chi_v, \chi_w$, which diagonalizes H_{SS}, H_Q^N and H_Q^{Cl}. τ_u $(u = x,y,z)$ is the electron spin function, χ_v $(v = x,y,z)$ is the nitrogen spin function and χ_w $(w = \pm 1/2, \pm 3/2)$ is the doubly degenerate chlorine spin function. The total spin of the system is 7/2 and therefore a Kramers doublet. Consequently there are only 18 energy levels for each of the molecular isotopes.

The similarity of the excited triplet state of 8-chloroquinoline and quinoline leads to the assignment of the order of the triplet energy levels of 8-chloroquinoline as being the same as those of quinoline.[58] (58) Therefore, with our axis system, the elements of H_{SS} are ordered $Y > Z > X$.

The nitrogen nuclear quadrupole energy levels are also assumed to be in the same order as those reported for the ground state of pyrazine and pyridine[59,60] (59, 60) and therefore, for H_Q^N, $x > y > z$.

Since the chlorine nuclear quadrupole coupling constant (e^2qQ) is negative for all covalently bonded Cl atoms, the energy of the chlorine spin functions are ordered $\chi_{\pm 1/2} > \chi_{\pm 3/2}$.

In order to treat the out-of-plane hyperfine perturbation due to both the nitrogen and chlorine spins, we will assume that the contribution from each may be considered separately. This is of course not strictly correct, but is satisfactory for the purpose of illustration, and in fact, for the value of A_{xx}^{N} and A_{xx}^{Cl} used in fitting the spectra, gives values for the energy levels very close to those obtained by diagonalizing the total spin Hamiltonian.

An energy level scheme using the perturbation method discussed in section III-D appropriate for 8-chloroquinoline is given in Figure 13.

There are essentially six types of ESR transitions observed,

A) electron spin,

B) electron and ^{14}N spins,

C) electron and ^{35}Cl spins,

D) electron and ^{37}Cl spins

E) electron, ^{14}N and ^{35}Cl spins

F) electron, ^{14}N and ^{37}Cl spins.

Since the chlorine nuclear quadrupole interaction is far larger than the nitrogen nuclear quadrupole interaction, the various types of transitions are easily identified. In Table 2 the measured and calculated frequencies are listed according to their type (A,B, etc.). In analyzing the spectra, the magnitude of the components of the spin Hamiltonian were first obtained by the perturbation method and final results by computer

diagonalization of the spin Hamiltonian. The ^{14}N and ^{35}Cl out-of-plane hyperfine elements were found to be approximately 19.5 and 15 MHz respectively. With only one nitrogen hyperfine element only one nitrogen quadrupole transition is observed corresponding to the in-plane $\chi_z \rightarrow \chi_y$ transition which was found to be 3.2 ± .2 MHz. With our assumption that the asymmetry parameter may be neglected the ^{35}Cl nuclear quadrupole coupling constant was found to be -68.4 ± 0.6 MHz.

The calculated frequencies listed in Table 2 were obtained by analysis of the components of the observed spectra due to the ^{35}Cl molecular isotope. The transitions associated with the molecules possessing the ^{37}Cl isotope were then obtained by using the same values for H_{SS}, $H_Q{}^N$ and $H_{HF}{}^N$ and correcting $H_Q{}^{Cl}$ for the difference in the nuclear quadrupole moments and $H_{HF}{}^{Cl}$ for the difference in the magnetogyric ratio of the two chlorine isotopes.

All calculated frequencies were obtained by collecting all transitions within 0.75 MHz of another and weighting each by its electron magnetic moment transition probability.

Although it is difficult to make a comprehensive analysis of the electron distribution in the excited triplet state without a measure of all the components of the hyperfine tensor, it is reasonable to make a few general observations. The similarity of the nitrogen nuclear quadrupole and hyperfine interactions in 8-chloroquinoline and quinoline and the observation that the chlorine nuclear quadrupole coupling constant is approximately the same as that reported for the ground state of 6-chloroquinoline (69.256 MHz) and 7-chloroquinoline (69.362 MHz)[61,62] further supports the assumption that the excited triplet state of 8-chloroquinoline is essentially the same as that of quinoline.

(61,62)

V. Acknowledgment

This work was supported by the Lawrence Radiation Laboratory (LRRD Division) under the auspices of the U. S. Atomic Energy Commission.

Table 1

Spin Hamiltonian parameters and triplet lifetimes of the $^3\pi\pi^*$ states of 8-chloroquinoline and quinoline.

	8-chloroquinoline in durene (1.3°K)	quinoline in durene (1.35°K)[a]
Y (MHz)	1414.5	1528.5
Z (MHz)	555.5	528.0
X (MHz)	-1970.0	-2056.5
D[b] (MHz)	2399.5	2556.75
E[b] (MHz)	-429.5	-500.25
A_{xx}^{N} (MHz)	19.5	22.[c]
A_{xx}^{Cl} (MHz)	15.	---
$e^2qQ(^{14}N)$[d] (MHz)	4.27	~ 4.0[e]
$e^2qQ(^{35}Cl)$ (MHz)	-68.4	---
τ_x (sec)	≥1	5.0
τ_y (sec)	0.11	0.32
τ_z (sec)	≥1	2.7

[a] data from reference 58

[b] with the definitions D = - 3/2X and E = - 1/2(Y-Z)

[c] data from reference 54

[d] with the assumptions $e^2qQ(^{14}N) = 4/3(y-z)$

[e] data from reference 26

Table 2

Measured and calculated ESR transitions of the $^3\pi\pi^*$ state of of 8-chloroquinoline

	Measured frequency (±0.5 MHz)	Calculated frequency	Classification
a) $\tau_x \rightarrow \tau_y$			
	3422.8	3422.7	E
	3419.5	3419.5	C
	3416.5	3416.5	E
	3415.3	3415.3	F
	3412.0	3412.1	D
	3409.3	3409.1	F
	3388.9	3388.3	B
	3385.9	3385.1	A
	3382.7	3382.2	B
	3361.2	3361.1	F
	3358.1	3358.0	D
	3354.5	3355.2	F
	3353.9	3353.9	E
	3350.9	3350.8	C
	3347.6	3348.0	E
b) $\tau_x \rightarrow \tau_z$			
	2562.3	2561.9	E
	2559.3	2558.9	C
	2555.8	2555.7 2554.8	E,F
	2552.3	2551.8	D
	2548.9	2548.6	F
	2525.5	2524.9	A
	2501.7	2500.9	F
	2498.0	2498.1	D
	2494.4	2493.6 2495.0	E,F
	2491.0	2490.8	C
	2487.9	2487.7	E
c) $\tau_z \rightarrow \tau_y$			
	898.1	897.9	E
	895.6	894.7	C
	891.7	891.6	E
	890.7	890.4	F
	888.2	887.3	D
	884.3	884.2	F
	863.8	864.1	B
	860.1	860.2	A
	857.3	857.4	B
	836.4	836.4	F
	833.5	833.4	D
	830.8	830.3	F
	829.8	829.4	E
	826.5	826.0	C
	822.9	823.2	E

References

1. S. P. McGlynn, T. Azumi and M. Kinoshito, Molecular Spectroscopy of the Triplet State (Prentice-Hall, Inc., 1969).
2. R. S. Becker, Theory and Interpretation of Fluorescence and Phosphorescence (Wiley Interscience, John Wiley & Sons, Inc., 1969).
3. S. K. Lower and M. A. El-Sayed, Chem. Rev., 66, 199 (1966).
4. M. S. DeGroot, I. A. M. Hesselmann and J. H. van der Waals, Mol. Phys. 12, 259 (1967).
5. G. N. Lewis and M. J. Kasha, J. Am. Chem. Soc. 66, 2100 (1944).
6. G. N. Lewis and M. J. Kasha, J. Am. Chem. Soc. 67, 994 (1945).
7. G. N. Lewis and M. Calvin, J. Am. Chem. Soc. 67, 1232 (1945).
8. G. N. Lewis, M. J. Kasha, and M. Calvin, J. Chem. Phys. 17, 804 (1949).
9. H. F. Hameka, thesis, Leiden (1956).
10. C. A. Hutchison and B. W. Mangum, J. Chem. Phys. 29, 952 (1958).
11. C. A. Hutchison and B. W. Mangum, J. Chem. Phys. 34, 908 (1961).
12. Ph. Kottis and R. Lefebvre, J. Chem. Phys. 39, 393 (1963).
13. Ph. Kottis and R. Lefebvre, J. Chem. Phys. 41, 379 (1964).
14. S. Geschwind, G. E. Devlin, R. L. Cohen, and S. R. Chinn, Phys. Rev 137, AL087 (1965).
15. J. Brossel and A. Kastler, Compt. Rend. 229, 1213 (1949).
16. J. Brossel and F. Bitter, Phys. Rev. 86, 308 (1952).
17. M. Sharnoff, J. Chem. Phys. 46, 3263 (1967).
18. A. L. Kwiram, Chem. Phys. Letters 1, 272 (1967).
19. J. Schmidt, I. A. M. Hesselmann, M. S. DeGroot and J. H. van der Waals, Chem. Phys. Letters 1, 434 (1967).
20. J. Schmidt and J. H. van der Waals, Chem. Phys. Letters 2, 640 (1968).
21. R. W. Brandon, R. E. Gerkin and C. A. Hutchison, Jr., J. Chem. Phys. 41, 3717 (1968).
22. J. Schmidt and J. H. van der Waals, Chem. Phys. Letters 3, 546 (1969).
23. D. S. Tinti, M. A. El-Sayed, A. H. Maki and C. B. Harris, Chem. Phys. Letters 3, 343 (1969).
24. C. B. Harris, D. S. Tinti, M. A. El-Sayed and A. H. Maki, Chem. Phys. Letters 4, 409 (1969).

25. I. Y. Chan, J. Schmidt and J. H. van der Waals, Chem. Phys. Letters 4, 269 (1969).
26. M. J. Buckley, C. B. Harris and A. H. Maki, Chem. Phys. Letters 4, 591 (1970).
27. M. J. Buckley and C. B. Harris, Chem. Phys. Letters 5, 205 (1970).
28. T. S. Kuan, D. S. Tinti and M. A. El-Sayed, Chem. Phys. Letters 4, 507 (1970).
29. C. B. Harris, J. Chem. Phys. 54, 972 (1971).
30. C. B. Harris, Proc. of 5th Molecular Crystals Symposium, Philadelphia (1970).
31. J. Schmidt, W. G. van Dorp and J. H. van der Waals, Chem. Phys. Letters 8, 345 (1971).
32. W. E. Bell and A. L. Bloom, Phys. Rev. 107, 1559 (1957).
33. L. L. Chase, Phys. Rev. Letters 21, 888 (1968).
34. W. S. Veeman and J. H. van der Waals, Chem. Phys. Letters 7, 65 (1970).
35. M. D. Mayer, D. A. Yuen and C. B. Harris, J. Chem. Phys. 53, 4719 (1970).
36. M. Schwoerer and H. C. Wolf, Molecular Crystals 3, 177 (1967).
37. D. Haarer and H. C. Wolf, Mol. Cryst. and Liq. Cryst. 10, 359 (1970).
38. M. Sharnoff, Symposium of the Faraday Society, No. 3, Magneto Optical Effects (1969).
39. A. H. Francis and C. B. Harris, Chem. Phys. Letters 9, 181 (1971); 9, 188 (1971).
40. M. A. El-Sayed, J. Chem. Phys. 54, 680 (1971).
41. M. A. El-Sayed, D. S. Tinti and E. M. Yee, J. Chem. Phys. 51, 5721 (169); M. A. El-Sayed, D. S. Tinti and O. V. Owens, Chem. Phys. Letters 3, 339 (1969); M. E. El-Sayed, J. Chem. Phys. 52, 6438 (1970); M. A. El-Sayed and O. F. Kalman, J. Chem. Phys. 52, 4903 (1970);
42. H. F. Hameka in The Triplet State (proc. International Symposium on the Triplet State, 1967) (Cambridge University Press, 1967) p. 25.
43. E. Gilmore, G. Gibson and D. McClure, J. Chem. Phys. 20, 829 (1952); 23, 399 (1955).
44. M. S. de Groot and J. H. van der Waals, Mol. Phys. 6, 545 (1963).

45. D. S. McClure, J. Chem. Phys. 17, 905 (1949).
46. M. J. Buckley and C. B. Harris, unpublished results.
47. M. Tinkham and M. W. P. Strandberg, Phys. Rev. 97, 937 (1955); M. Gouterman and W. Moffitt, J. Chem. Phys. 30, 1107 (1959).
48. A. Carrington and A. D. McLachlan, Introduction to Magnetic Resonance (Harper and Row, 1967), p. 117.
49. T. P. Das and E. L. Hahn, Nuclear Quadrupole Resonance Spectroscopy, (Academic Press, New York/London, 1958); M. H. Cohen and F. Reif, Solid State Physics V. 5 (Academic Press, New York/London, 1957); E. A. C. Lucken, Nuclear Quadrupole Coupling Constants (Academic Press, New York/London, 1969).
50. R. H. Webb, Rev. Sci. Instr. 33, 732 (1962).

51. M. Kasha, J. Opt. Sci. Am., 38, 929 (1948).
52. D. Owens, M. A. El-Sayed and S. Ziegler, J. Chem. Phys. 52, 4315 (1970).
53. C. A. Hutchison Jr., J. V. Nicholas and G. W. Scott, J. Chem. Phys. 53, 1906 (1970).
54. J. S. Vincent and A. H. Maki, J. Chem. Phys. 42, 865 (1965).
55. Y. Gondo and A. H. Maki, J. Chem. Phys. 50, 3270 (1969).
56. D. Pooley and D. H. Wiffen, Spectrochimica Acta, 18, 291 (1962).
57. H. R. Falle, G. R. Luckhurst, A. Horsfield and M. Ballester, J. Chem. Phys. 50, 258 (1969).
58. J. Schmidt, W. S. Veeman and J. H. van der Waals, Chem. Phys. Letters 4, 341 (1969).
59. E. A. C. Lucken, Trans. Faraday Soc. 57, 729 (1961).
60. E. Schempp and P. J. Bray, J. Chem. Phys. 46, 1186 (1967).
61. S. L. Segal, R. G. Barnes and P. J. Bray, J. Chem. Phys. 25, 1286 (1956).
62. M. Dewar and E. Lucken, J. Chem. Soc. (London), 2653 (1958).

Figure Captions

Fig. 1 Relaxation pathways and rate constants for the triplet state.

Fig. 2 Relaxation pathways and rate constants considering only two of the three triplet levels (see text).

Fig. 3 Population change predicted for ESR ($b \leftrightarrow d$) and ENDOR ($a \leftrightarrow b$) transitions.

Fig. 4 Energy level diagram for the triplet and one $I = 1$ nuclear spin considering only the A_{xx} hyperfine component.

Fig. 5 ODMR spectra predicted for the energy level diagram shown in Fig. 4.

Fig. 6 Energy level diagram for the triplet and one $I = 3/2$ nuclear spin considering only the A_{xx} hyperfine component.

Fig. 7 ODMR spectra predicted for the energy level diagram shown in Fig. 6.

Fig. 8 Energy level diagram for the triplet and one $I = 3/2$ nuclear spin considering only the A_{zz} hyperfine component.

Fig. 9 ODMR spectra predicted for the energy level diagram shown in Fig. 8.

Fig. 10 Experimental arrangement used in performing ODMR experiments in zero field with amplitude modulation of the microwave field.

Fig. 11 The $\tau_x \rightarrow \tau_y$, $\tau_x \rightarrow \tau_z$ and $\tau_z \rightarrow \tau_y$ optically detected ESR transitions in 8-chloroquinoline using relatively high microwave power. The $\tau_x \rightarrow \tau_z$ transition was obtained by performing an EEDOR experiment.

Fig. 12 Optically detected ^{35}Cl ENDOR observed while saturating the $\tau_y \rightarrow \tau_z$ multiplet.

Fig. 13 Energy level diagram for 8-chloroquinoline.

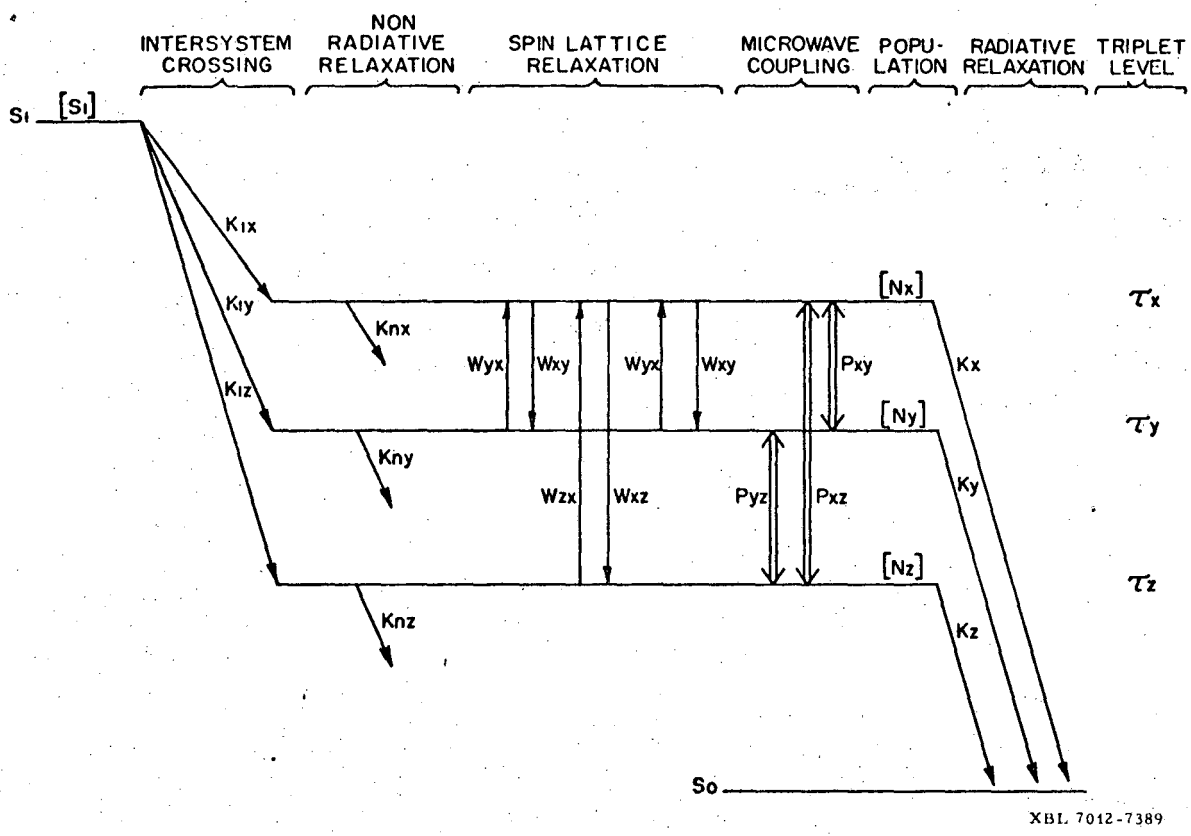
INTERSYSTEM CROSSING
NON RADIATIVE RELAXATION
SPIN LATTICE RELAXATION
MICROWAVE COUPLING
POPU-LATION
RADIATIVE RELAXATION
TRIPLET LEVEL
S1
[S1]
K1x
K1y
K1z
Knx
Kny
Knz
Wyx
Wxy
Wyx
Wxy
Wzx
Wxz
Pyz
Pxz
Pxy
[Nx]
[Ny]
[Nz]
Kx
Ky
Kz
τx
τy
τz
So
XBL 7012-7389

Fig. 1

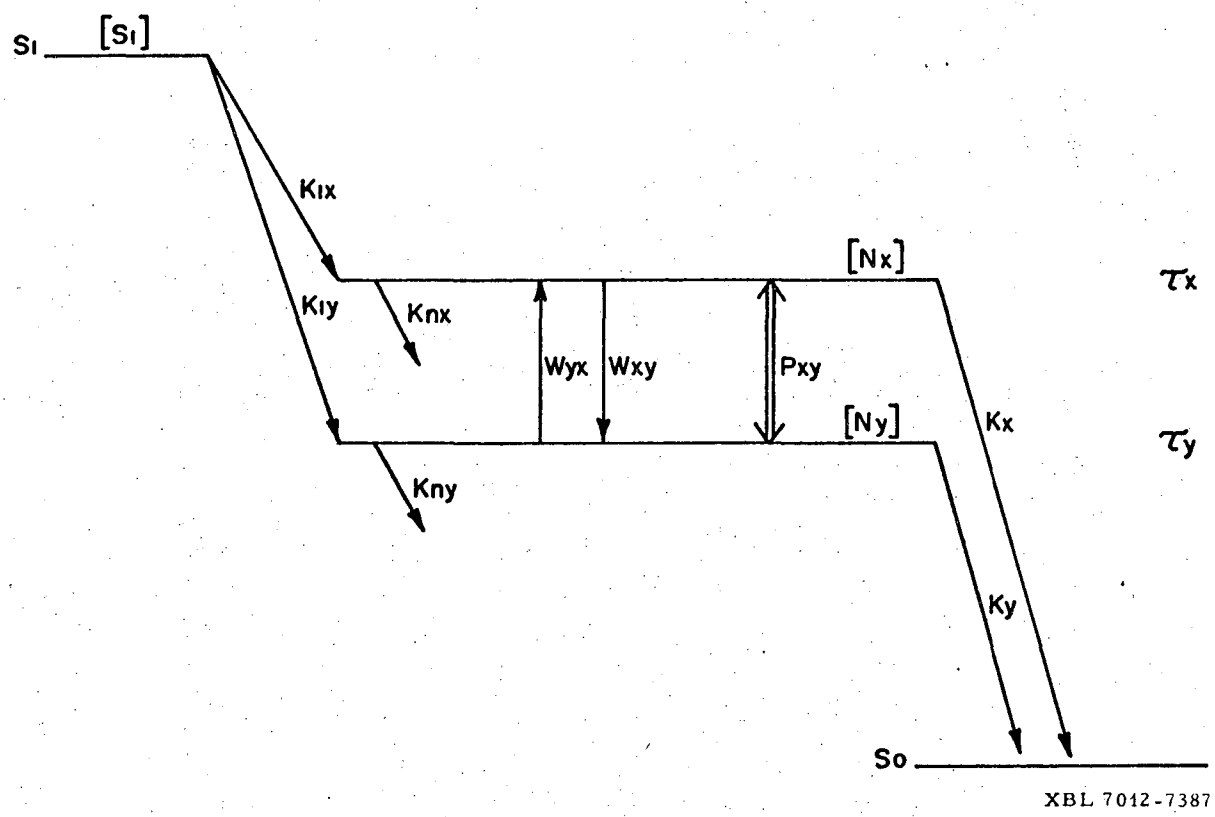
Si
[Si]
Kix
Kiy
Knx
Wyx
Wxy
Pxy
[Nx]
[Ny]
Kx
Ky
Kny
So
τx
τy
XBL 7012-7387

Fig. 2

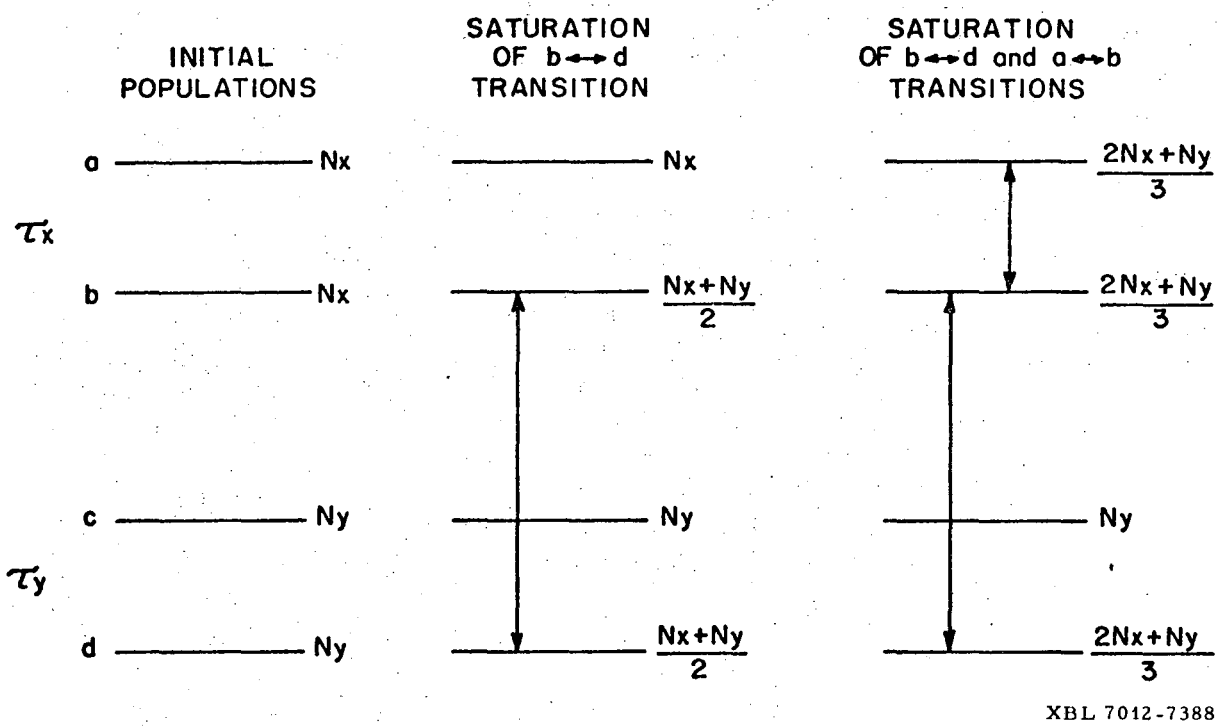
INITIAL POPULATIONS
SATURATION OF b↔d TRANSITION
SATURATION OF b↔d and a↔b TRANSITIONS
a
b
c
d
Nx
Nx
Ny
Ny
τx
τy
Nx
Nx+Ny/2
Ny
Nx+Ny/2
2Nx+Ny/3
2Nx+Ny/3
Ny
2Nx+Ny/3
XBL 7012-7388

Fig. 3

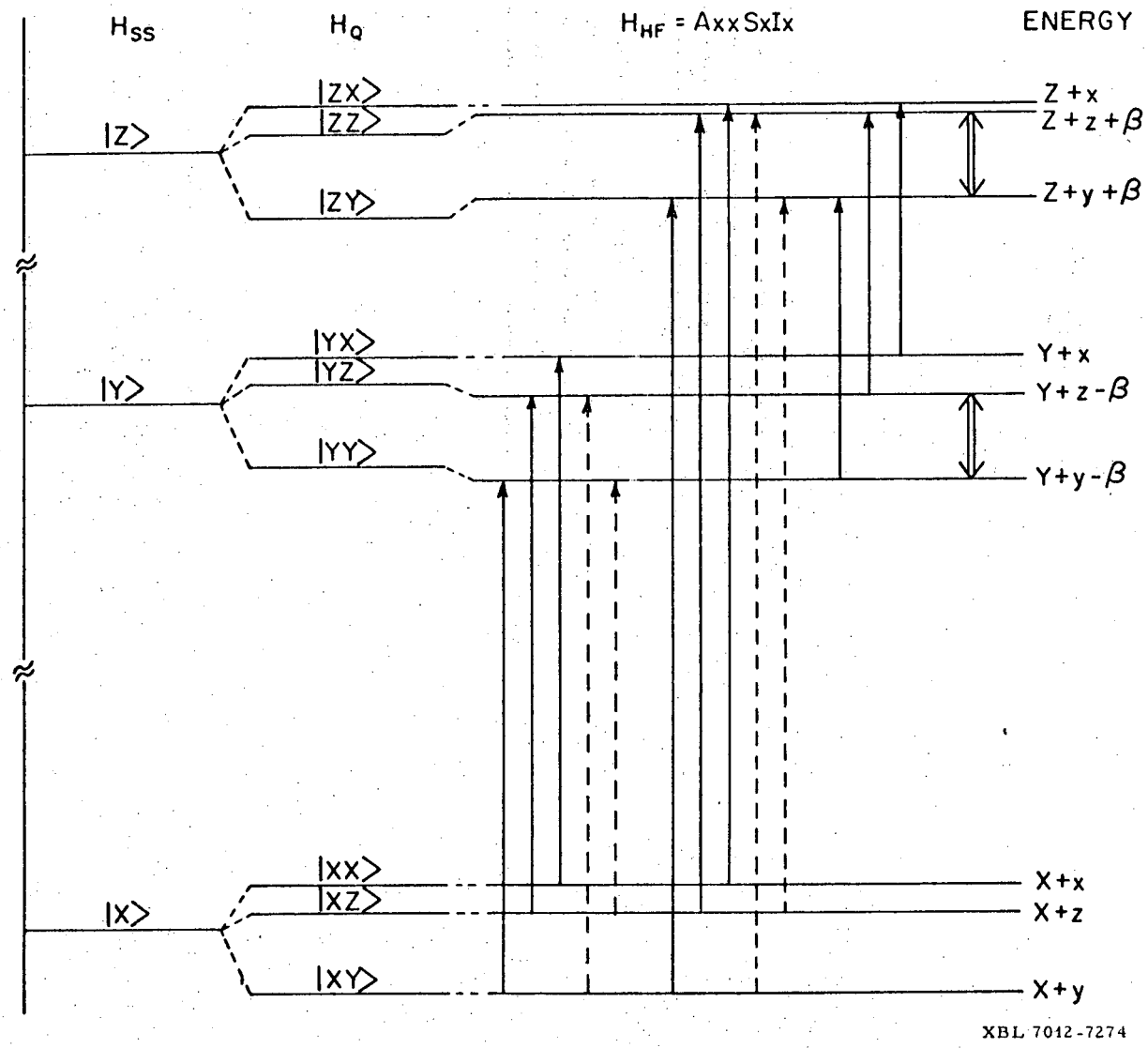
H_{SS}
H_Q
$H_{HF} = AxxSxIx$
ENERGY
|Z>
|ZX>
|ZZ>
|ZY>
Z + x
Z + z + β
Z + y + β
|Y>
|YX>
|YZ>
|YY>
Y + x
Y + z - β
Y + y - β
|X>
|XX>
|XZ>
|XY>
X + x
X + z
X + y
XBL 7012-7274

Fig. 4

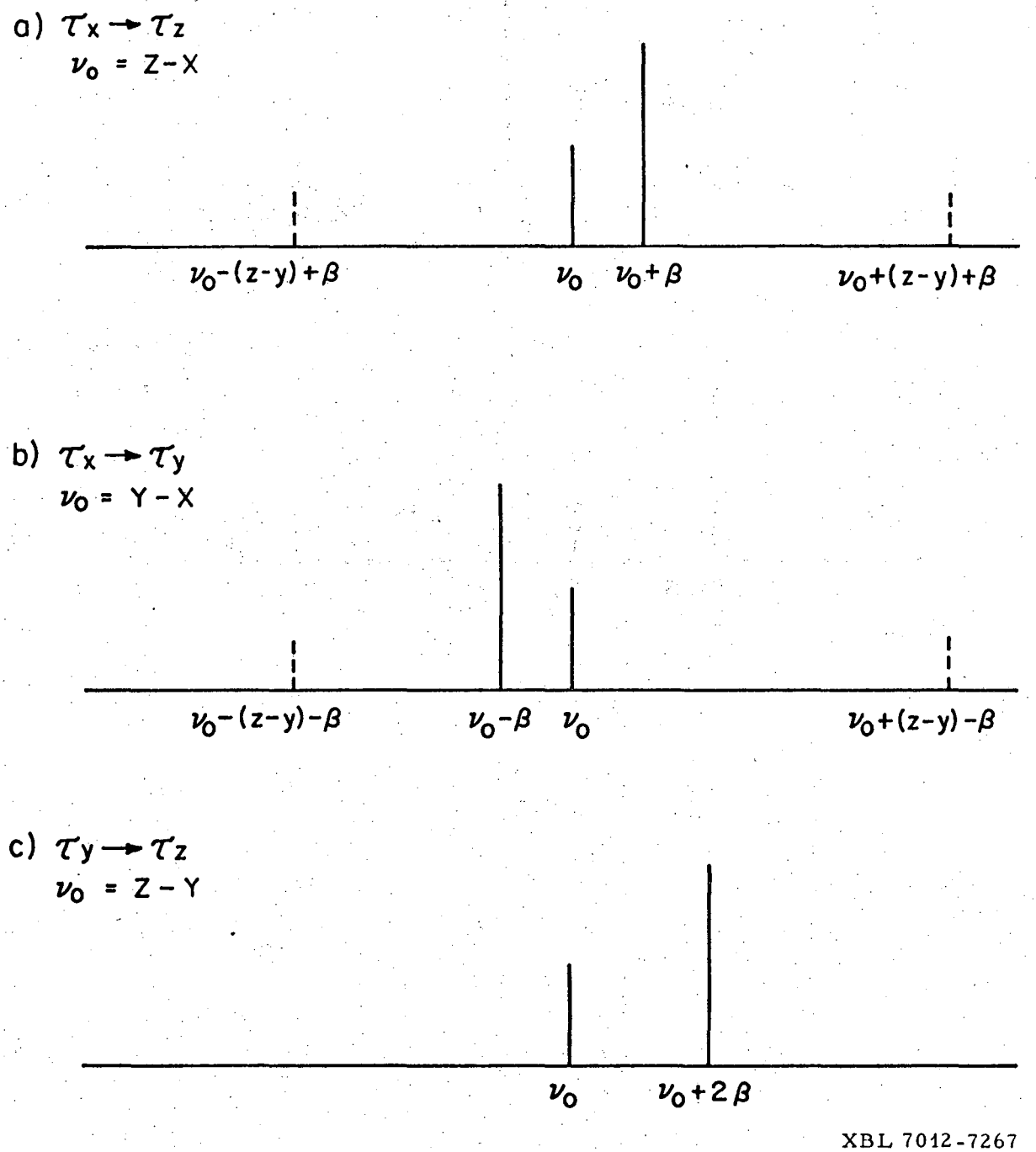
a) $\tau_x \rightarrow \tau_z$
$\nu_o = Z - X$
$\nu_o - (z-y) + \beta$
ν_o
$\nu_o + \beta$
$\nu_o + (z-y) + \beta$
b) $\tau_x \rightarrow \tau_y$
$\nu_o = Y - X$
$\nu_o - (z-y) - \beta$
$\nu_o - \beta$
ν_o
$\nu_o + (z-y) - \beta$
c) $\tau_y \rightarrow \tau_z$
$\nu_o = Z - Y$
ν_o
$\nu_o + 2\beta$
XBL 7012-7267

Fig. 5

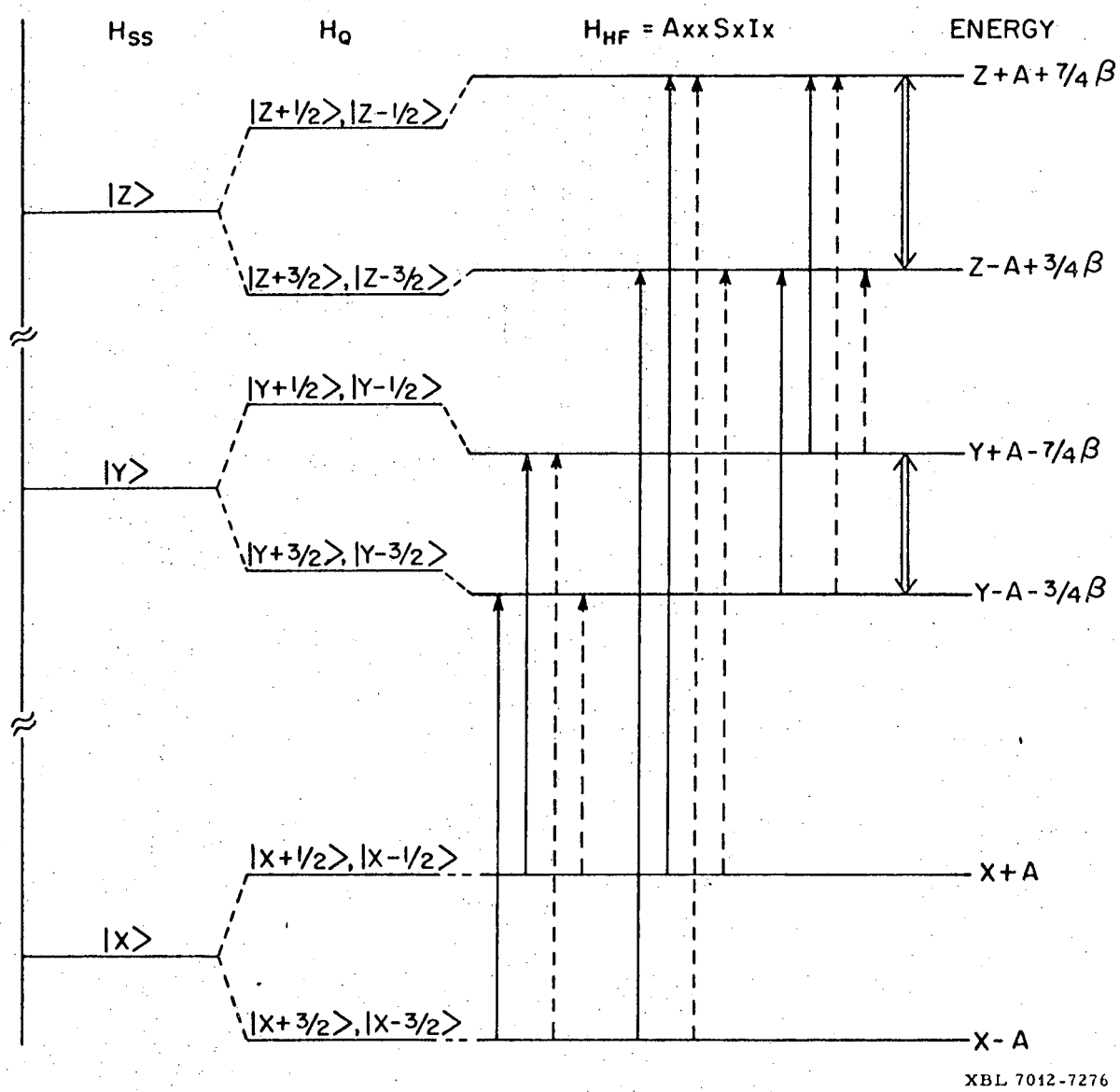
H_{SS}
H_Q
$H_{HF} = AxxSxIx$
ENERGY
$|Z\rangle$
$|Z+1/2\rangle, |Z-1/2\rangle$
$|Z+3/2\rangle, |Z-3/2\rangle$
$|Y\rangle$
$|Y+1/2\rangle, |Y-1/2\rangle$
$|Y+3/2\rangle, |Y-3/2\rangle$
$|X\rangle$
$|X+1/2\rangle, |X-1/2\rangle$
$|X+3/2\rangle, |X-3/2\rangle$
$Z+A+7/4\beta$
$Z-A+3/4\beta$
$Y+A-7/4\beta$
$Y-A-3/4\beta$
$X+A$
$X-A$
XBL 7012-7276

Fig. 6

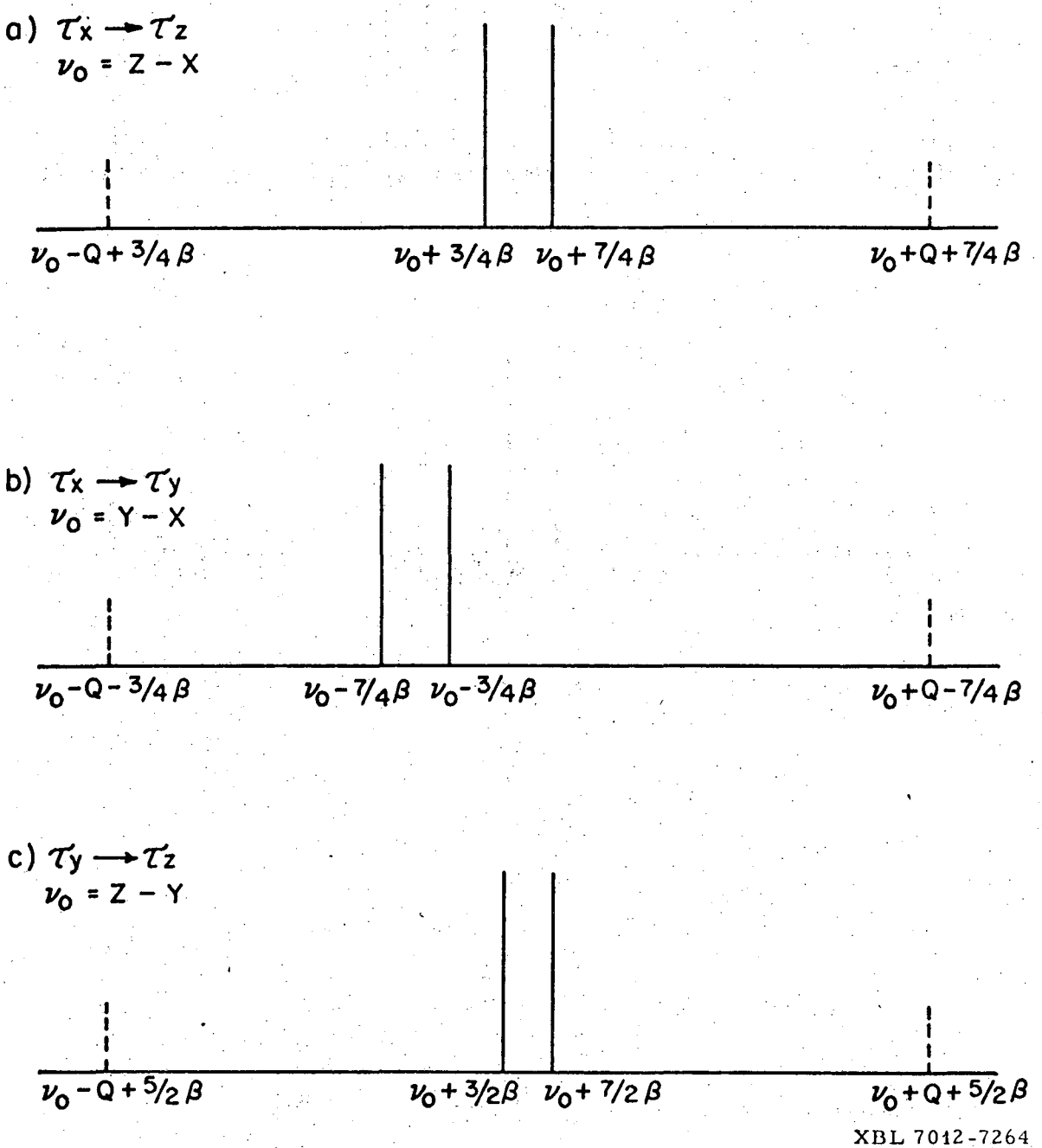
a) $\tau_x \rightarrow \tau_z$
$\nu_0 = Z - X$
$\nu_0 - Q + 3/4\,\beta$
$\nu_0 + 3/4\,\beta$
$\nu_0 + 7/4\,\beta$
$\nu_0 + Q + 7/4\,\beta$
b) $\tau_x \rightarrow \tau_y$
$\nu_0 = Y - X$
$\nu_0 - Q - 3/4\,\beta$
$\nu_0 - 7/4\,\beta$
$\nu_0 - 3/4\,\beta$
$\nu_0 + Q - 7/4\,\beta$
c) $\tau_y \rightarrow \tau_z$
$\nu_0 = Z - Y$
$\nu_0 - Q + 5/2\,\beta$
$\nu_0 + 3/2\beta$
$\nu_0 + 7/2\,\beta$
$\nu_0 + Q + 5/2\,\beta$
XBL 7012-7264

Fig. 7

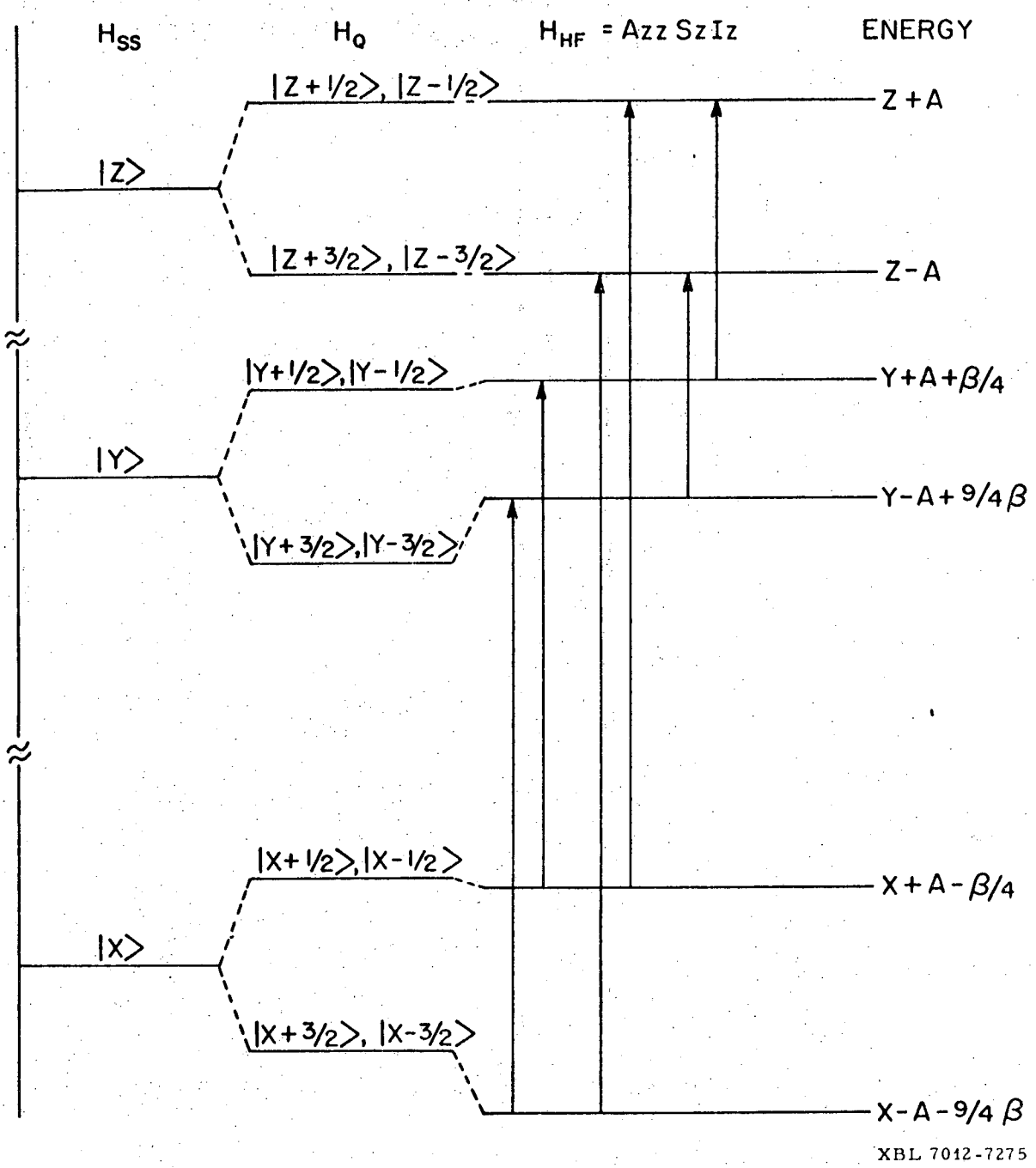
H_{SS}
H_Q
$H_{HF} = Azz\ Sz\ Iz$
ENERGY
|Z+1/2>, |Z-1/2>
|Z>
|Z+3/2>, |Z-3/2>
Z+A
Z-A
|Y+1/2>, |Y-1/2>
|Y>
|Y+3/2>, |Y-3/2>
Y+A+β/4
Y-A+9/4β
|X+1/2>, |X-1/2>
|X>
|X+3/2>, |X-3/2>
X+A-β/4
X-A-9/4β
XBL 7012-7275

Fig. 8

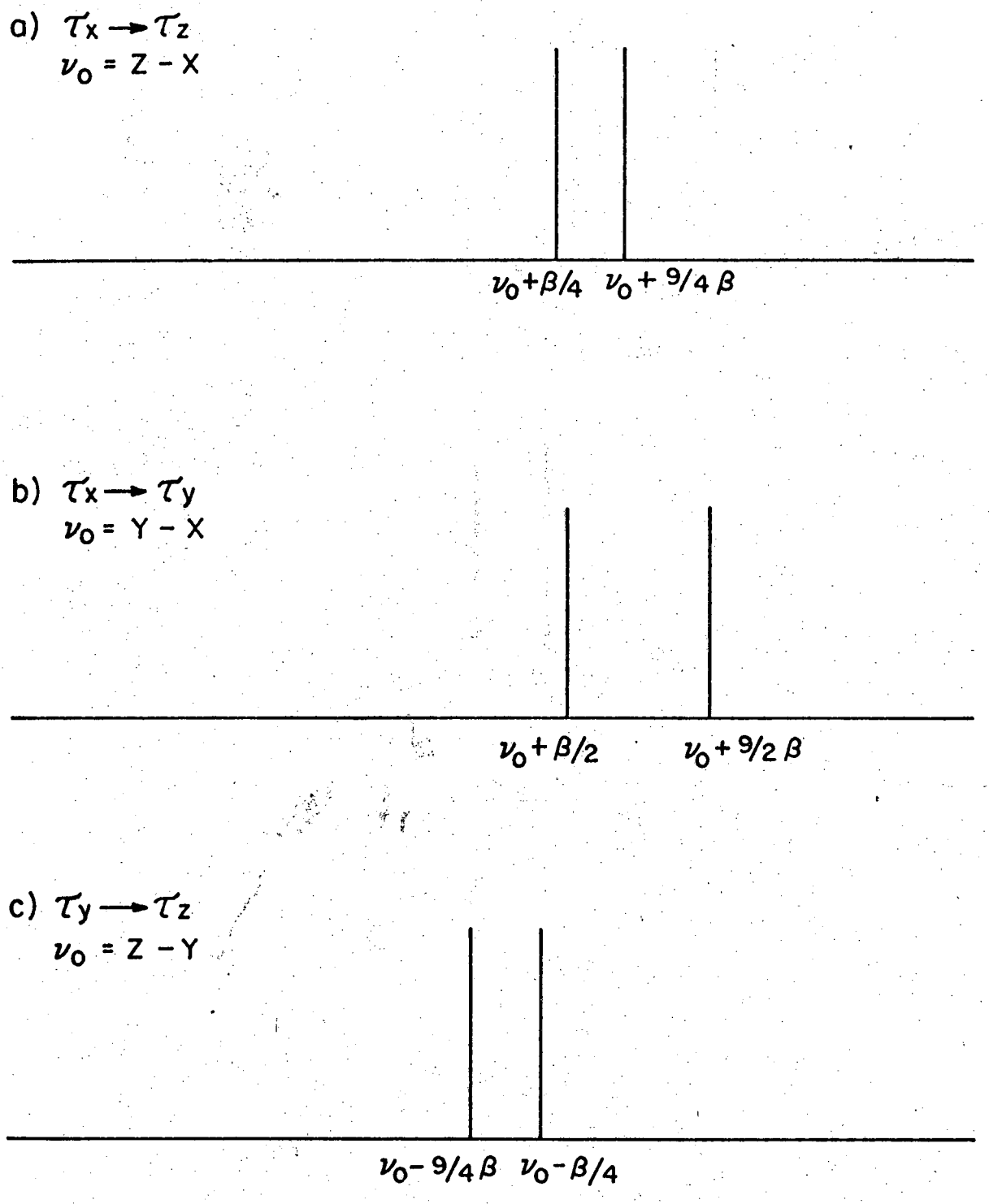

XBL 7012-7268

Fig. 9

ESR EXPERIMENT

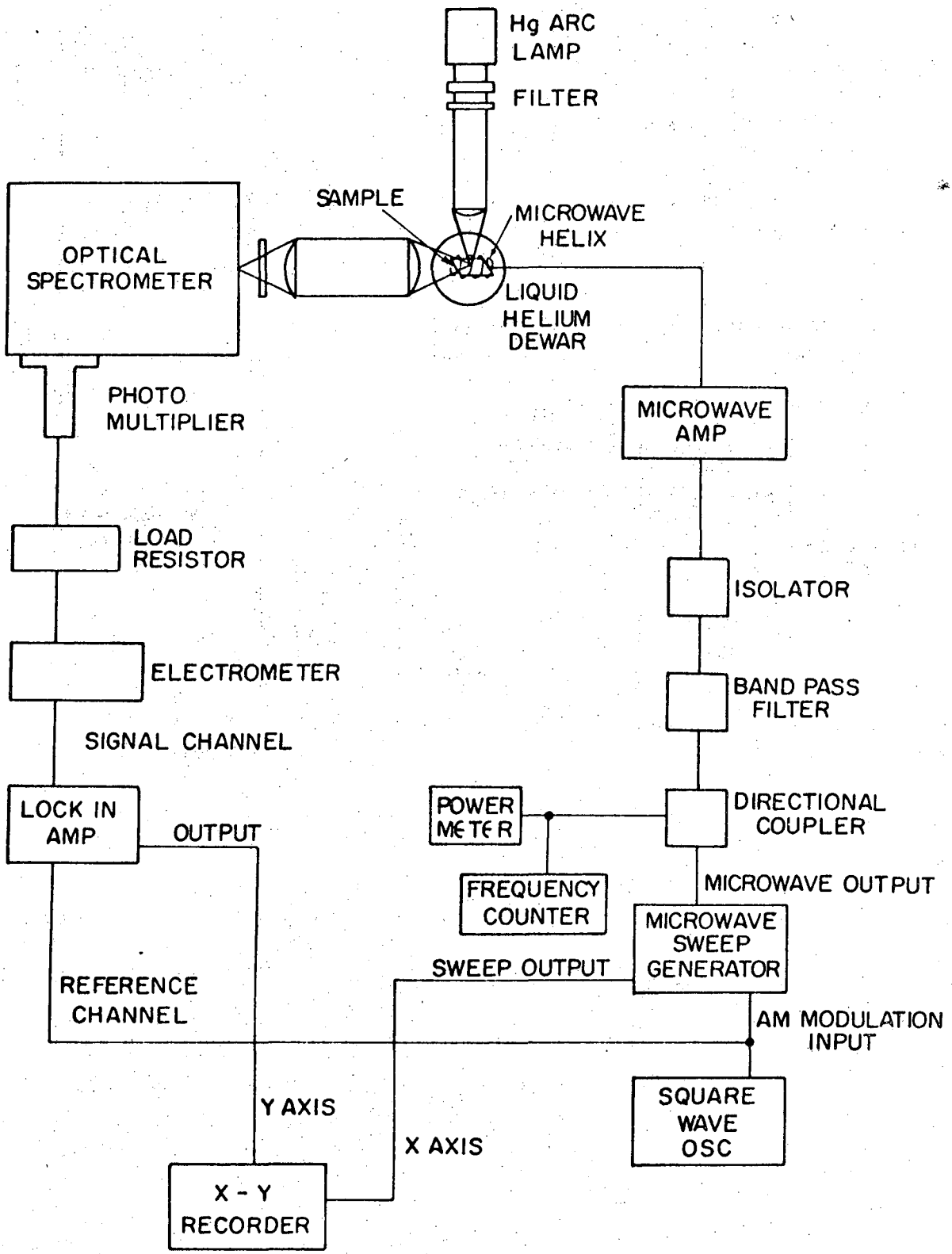

Fig. 10

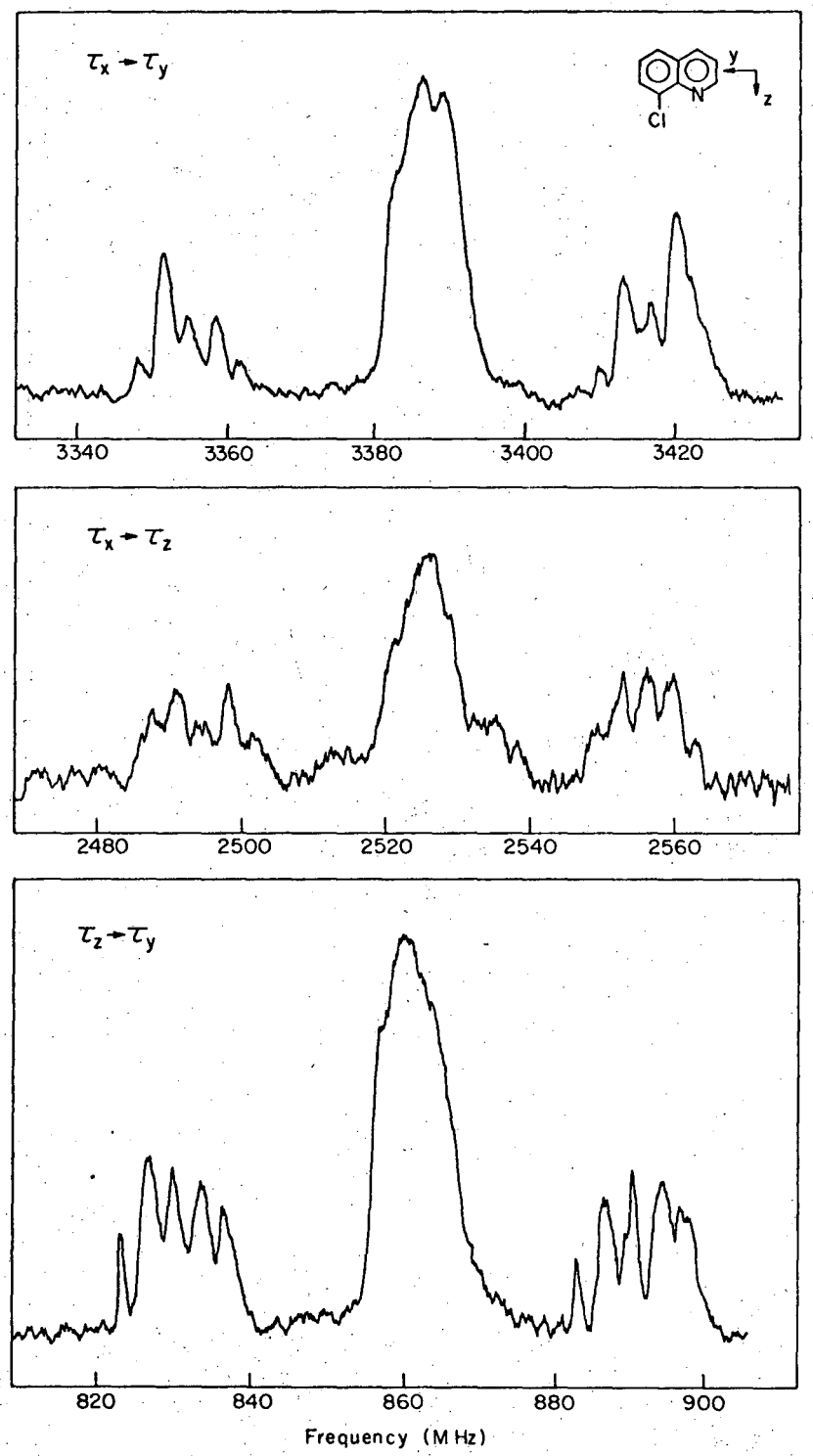

XBL716-6866

Fig. 11

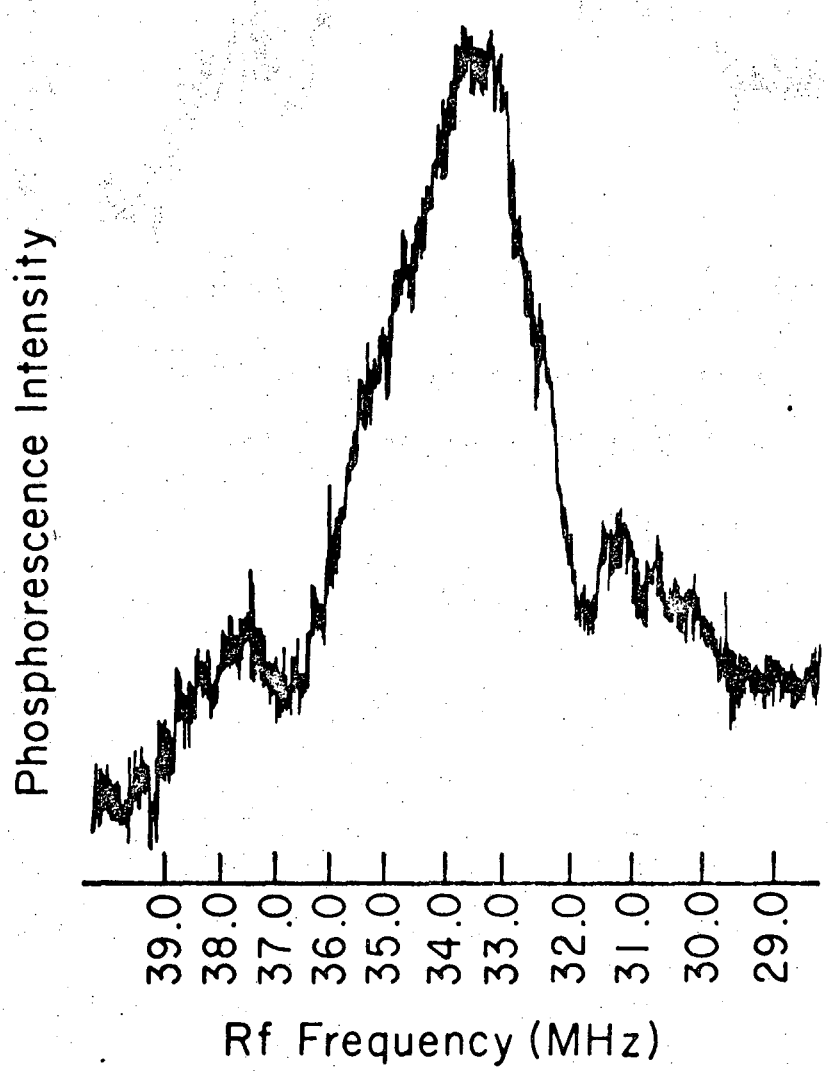

XBL 717-7086

Fig. 12

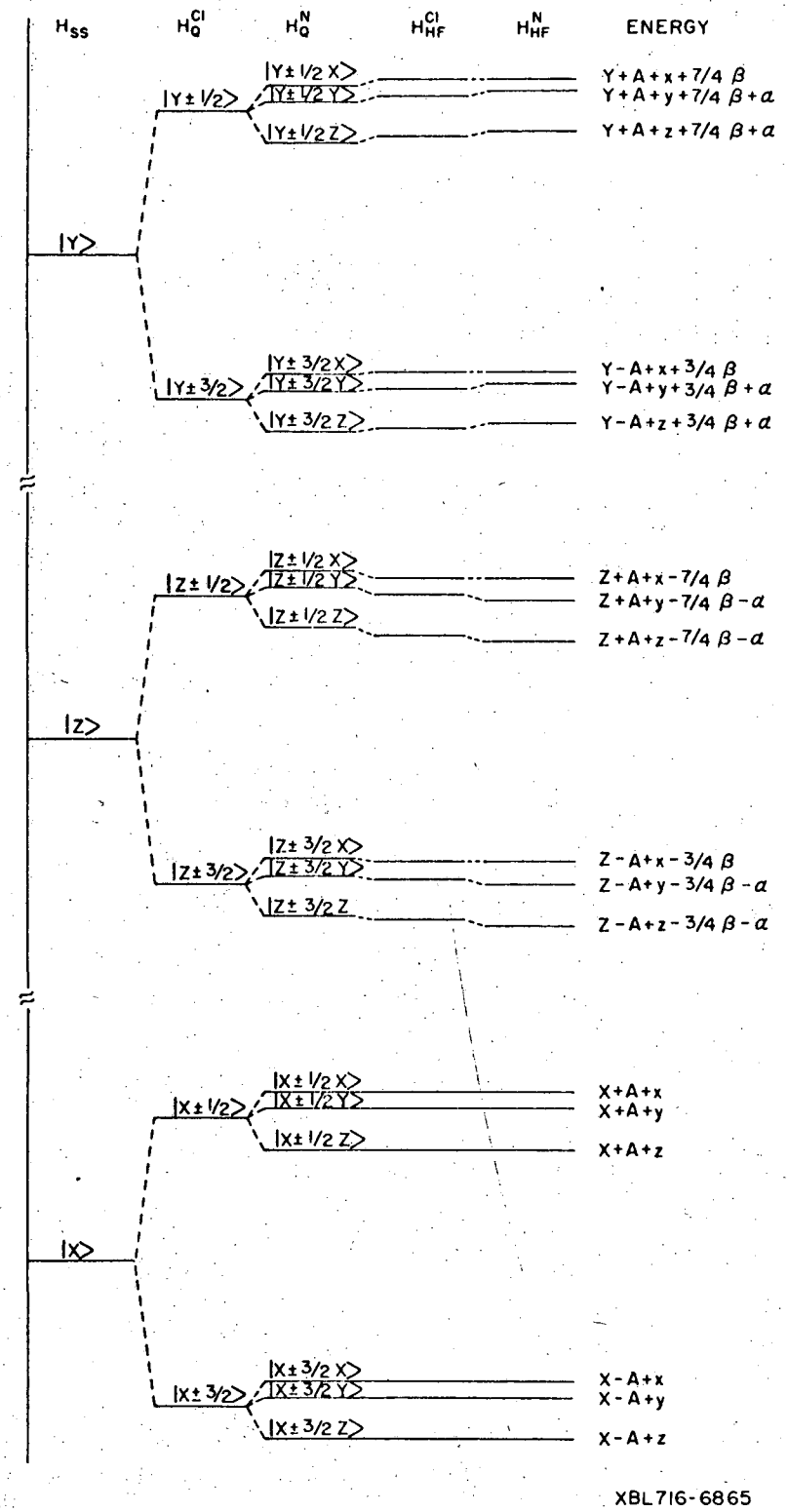
H_{SS}
H_Q^{Cl}
H_Q^N
H_{HF}^{Cl}
H_{HF}^N
ENERGY
|Y>
|Y ± 1/2>
|Y ± 1/2 X>
|Y ± 1/2 Y>
|Y ± 1/2 Z>
Y + A + x + 7/4 β
Y + A + y + 7/4 β + α
Y + A + z + 7/4 β + α
|Y ± 3/2>
|Y ± 3/2 X>
|Y ± 3/2 Y>
|Y ± 3/2 Z>
Y - A + x + 3/4 β
Y - A + y + 3/4 β + α
Y - A + z + 3/4 β + α
|Z>
|Z ± 1/2>
|Z ± 1/2 X>
|Z ± 1/2 Y>
|Z ± 1/2 Z>
Z + A + x - 7/4 β
Z + A + y - 7/4 β - α
Z + A + z - 7/4 β - α
|Z ± 3/2>
|Z ± 3/2 X>
|Z ± 3/2 Y>
|Z ± 3/2 Z>
Z - A + x - 3/4 β
Z - A + y - 3/4 β - α
Z - A + z - 3/4 β - α
|X>
|X ± 1/2>
|X ± 1/2 X>
|X ± 1/2 Y>
|X ± 1/2 Z>
X + A + x
X + A + y
X + A + z
|X ± 3/2>
|X ± 3/2 X>
|X ± 3/2 Y>
|X ± 3/2 Z>
X - A + x
X - A + y
X - A + z
XBL716-6865

Fig. 13

TECHNICAL INFORMATION DIVISION
LAWRENCE BERKELEY LABORATORY
UNIVERSITY OF CALIFORNIA
BERKELEY, CALIFORNIA 94720